# TabMGP: Martingale Posterior with TabPFN

Kenyon Ng kenyon.ng@monash.edu

Department of Econometrics and Business Statistics, Monash University

Edwin Fong chefong@hku.hk

Department of Statistics and Actuarial Science, The University of Hong Kong

David T. Frazier david.frazier@monash.edu

Department of Econometrics and Business Statistics, Monash University

 $\textbf{Jeremias Knoblauch} \hspace{1.5cm} \textit{j.knoblauch@ucl.ac.uk} \hspace{1.5cm} \textit{j.knoblauch@ucl.ac.uk}$ 

Department of Statistical Science, University College London

Susan Wei susan.wei@monash.edu

Department of Econometrics and Business Statistics, Monash University

#### **Abstract**

Bayesian inference provides principled uncertainty quantification but is often limited by challenges of prior elicitation, likelihood misspecification, and computational burden. The martingale posterior (MGP, Fong et al., 2023) offers an alternative, replacing prior–likelihood elicitation with a predictive rule — namely, a sequence of one-step-ahead predictive distributions — for forward data generation. The utility of MGPs depends on the choice of predictive rule, yet the literature has offered few compelling examples. Foundation transformers are well-suited here, as their autoregressive generation mirrors this forward simulation and their general-purpose design enables rich predictive modeling. We introduce TabMGP, an MGP built on TabPFN, a transformer foundation model that is currently state-of-the-art for tabular data. TabMGP produces credible sets with near-nominal coverage and often outperforms both existing MGP constructions and standard Bayes.

#### 1 Introduction

Bayesian inference provides a principled framework for uncertainty quantification, but its classical formulation hinges on the specification of a prior–likelihood pair. This requirement can be burdensome in practice. Priors are often placed on uninterpretable parameters, and "uninformative" defaults can dominate inference in data-scarce or high-dimensional regimes (Zhang et al., 2022). The problem is further compounded by the fact that the likelihood itself is often misspecified in modern applications. These limitations have motivated a wave of generalisations – ranging from generalised Bayes (Bissiri et al., 2016) to optimisation-centric Bayes (see e.g. Knoblauch et al., 2022; Wild et al., 2023; Shen et al., 2025) that modernise parts of the Bayesian recipe. Collectively, they mark the emergence of a post-Bayesian paradigm in statistical inference.

The martingale posterior represents one direction of this expansion. Originating in the Bayesian predictive literature (Fortini and Petrone, 2020; Berti et al., 2021; Fong et al., 2023), the martingale posterior shifts the focus from prior specification to prediction. Instead of eliciting a prior over parameters, the analyst provides a **predictive rule**, defined as a sequence of one-step-ahead predictive distributions. When such predictive rules satisfy certain technical conditions — namely, the martingale property — the resulting posterior is guaranteed to exist and be well-behaved (formal definition in Section 2). Posterior inference is then obtained by **forward sampling**: starting from the observed dataset, one repeatedly draws the next observation from the predictive rule conditional on the data so far, append it to the dataset, and continue.

The Bayesian predictive approach is particularly attractive in the modern era of powerful black-box predictive models, especially foundation transformers (Bommasani et al., 2022). In fact, the forward sampling mechanism described above will be familiar from large language models (LLMs): the predictive rule plays the role of next-token prediction, and forward sampling mirrors autoregressive generation, where at each step a token is sampled from the conditional distribution given the context, appended to the context, and the process is repeated. In this sense, transformers are naturally aligned with the forward-sampling procedure that underpins the martingale posterior. Furthermore, pretrained foundation models are explicitly designed to deliver accurate predictions across broad domains without bespoke modelling, making them natural candidates for predictive rules.

Yet, despite this alignment, the martingale posterior literature has focused almost exclusively on handcrafted predictive rules that satisfy exact martingale properties (e.g., Fong et al., 2023; Ghalebikesabi et al., 2023; Huk et al., 2024); see Section 4 for a review. These approaches are elegant, but they require problem-specific design choices and often impose strong conditions. In addition, the emphasis on exact martingale structure risks overstating its importance: the martingale property is sufficient to guarantee the existence of a limiting law and a well-defined martingale posterior, but it is not clear that it is necessary for delivering meaningful expressions of uncertainty about unknown parameters.

This motivates our central question: can modern predictive rules be used as the predictive rule in martingale posteriors? We answer in the affirmative by introducing **TabMGP**, the first martingale posterior powered by a large pretrained foundation transformer. Specifically, we instantiate the predictive rule with **TabPFN** (Hollmann et al., 2022; 2025), a transformer trained on a broad range of synthetic tabular data that now achieves state-of-the-art results for tabular classification and regression tasks. This integration yields several benefits:

- Off-the-shelf adaptivity: TabMGP requires no bespoke design of predictive rules or task-specific fitting.
- Scalability and generality: TabMGP applies broadly across regression and classification tasks, requiring only the specification of a loss functional.

Our results show that TabMGP consistently provides reliable uncertainty quantification, often matching or surpassing both handcrafted martingale posteriors and classical Bayesian inference. This establishes a practical new method for the modern Bayesian's toolkit and open new avenues and questions for broadening the martingale posterior framework.

# 2 Martingale posterior

The martingale posterior (Fong et al., 2023) is a recently proposed statistical inference method within the predictive Bayesian inference framework (see Fortini and Petrone, 2025, for a review). We largely follow the notation of Fortini and Petrone (2025) in our review of the martingale posterior framework below.

**Notation.** Let  $(Z_i)_{i\geq 1}$  be random variables taking values in a space  $\mathcal{Z}$ . For any probability law  $\mathbb{P}$  for the sequence  $(Z_i)_{i\geq 1}\in \mathcal{Z}^{\infty}$ , define the *predictive rule* as the sequence of predictive distribution  $P_0(\cdot):=\mathbb{P}(Z_1\in \cdot)$  and, for  $i\geq 1$ ,

$$P_i(\cdot) := \mathbb{P}(Z_{i+1} \in \cdot \mid Z_{1:i}).$$

We write  $P_i(\cdot \mid z_{1:i})$  for the realisation given  $z_{1:i}$ . We also write  $\mathbb{P}$ -a.s. for "with  $\mathbb{P}$ -probability one". We use p to denote the probability density or mass function of P; for example,  $p_i$  is the density or mass function of  $P_i$ .

The martingale posterior requires two ingredients:

- 1. A predictive rule  $(P_i)_{i>0}$ ; and
- 2. A functional of interest  $\theta : \mathcal{P}(\mathcal{Z}) \to \Theta \subseteq \mathbb{R}^p$ , where  $\mathcal{P}(\mathcal{Z})$  denotes the set of all probability distributions F on  $\mathcal{Z}$ .

In this work, we focus on a risk minimiser that minimises a given loss function  $\ell: \mathcal{Z} \times \Theta \to \mathbb{R}$ :

$$\theta(F) := \underset{\vartheta \in \Theta}{\operatorname{arg\,min}} \int \ell(z, \vartheta) \, \mathrm{d}F(z) \,. \tag{1}$$

For the martingale posterior distribution to be well-defined, the sequence of predictive distributions  $(P_i)_{i\geq 0}$  must converge  $\mathbb P$ -a.s. to a random probability measure  $F_{\infty}$ , which represents the limiting empirical distribution of  $(Z_i)_{i\geq 1}$ . The probability law of  $F_{\infty}$  can be regarded as a prior distribution and the probability law of  $F_{\infty} \mid z_{1:n}$  a posterior distribution. This posterior law of  $F_{\infty} \mid z_{1:n}$  then induces a posterior distribution on functionals of  $F_{\infty}$  which is termed the martingale posterior.

**Definition.** Let  $z_{1:n} \in \mathcal{Z}^n$  denote the observed data and  $\Pi(F_{\infty} \mid z_{1:n})$  the posterior law of  $F_{\infty}$  given  $z_{1:n}$ . The martingale posterior distribution is defined as the posterior law of  $\theta(F_{\infty})$ :

$$\Pi_{\infty}(\theta(F_{\infty}) \in A \mid z_{1:n}) = \int \mathbf{1}(\theta(F_{\infty}) \in A) \, d\Pi(F_{\infty} \mid z_{1:n}), \qquad (2)$$

for all measurable sets  $A \subseteq \Theta$ . The classical Bayesian posterior can be recovered from (2) as a special case by using a Bayesian posterior predictive distribution (PPD) as the predictive rule and the corresponding negative log-likelihood as the loss function; see Appendix B for details.

Sufficient conditions A sufficient, but not necessary, condition for the existence of  $F_{\infty}$  and hence for the martingale posterior distribution to be well-defined, is that the sequence  $(P_i)_{i\geq 0}$  is a martingale, or equivalently, that the sequence  $(Z_i)_{i\geq 1}$  is conditionally identically distributed (c.i.d, Berti et al., 2004). The martingale property stipulates that  $(P_i)_{i\geq 0}$  satisfies, for every  $i\geq 0$  and every measurable set A:

$$\mathbb{E}(P_{i+1}(A) \mid Z_{1:i}) = P_i(A). \tag{3}$$

Relaxations of this sufficient condition remain an active area of research (see, e.g., Battiston and Cappello, 2025). As noted in the introduction, the term martingale posterior is somewhat of a misnomer. Any predictive rule with a well-defined  $F_{\infty}$  limit induces a posterior distribution as in (2). In this paper, we use the term martingale posterior in a broad sense: even predictive rules that violate the martingale property may still induce valid "martingale" posteriors.

**Computation.** The martingale posterior (2) generally does not admit a closed-form expression and must be approximated by a *finite martingale posterior*, which is the posterior law of  $\theta(F_N)$  where  $F_N$  is the empirical distribution of  $Z_{1:N}$ . A sample from the finite martingale posterior can then be obtained as follows:

1. Starting from  $z_{1:n}$ , sequentially forward sample future observations  $Z_{n+1:N}$  for some large N:

$$Z_{i+1} \sim P_i, \quad i = n, \dots, N-1;$$

2. Form  $F_N$  and compute  $\theta(F_N)$ .

This procedure for generating a sample from the martingale posterior is known as predictive resampling (Fong et al., 2023). To approximate the (finite) martingale posterior, we repeat predictive resampling to obtain L samples  $\{\theta^{(l)}\}_{l=1}^L$ . The computation of these samples is embarrassingly parallelisable, as predictive resampling can be carried out independently for each sample.

#### 3 TabMGP

Given the strong predictive performance of modern foundation models (Bommasani et al., 2022), it is natural to ask whether such models can serve as a predictive rule in the martingale posterior framework. We describe our proposed methodology which employs TabPFN (Hollmann et al., 2022; 2025) as the predictive rule.

Given that TabPFN is designed for supervised prediction, we specialise the martingale posterior framework to the supervised setting, where each observation is a feature–response pair z = (x, y). In this setting, a predictive rule generates future pairs  $Z_{n+1}, \ldots, Z_N$ . Fong et al. (2023) describe this as the "joint method," which requires modelling both the distribution of X and the conditional distribution  $Y \mid X$ . Because modelling X can be challenging even in moderate dimensions, we follow Fong et al. (2023) and use the Bayesian bootstrap (see Section 4) to forward sample features, drawing  $X_{i+1}$  at random from the empirical distribution of  $x_{1:i}$ . In our work, we adopt this strategy for X, while TabPFN supplies the conditional  $Y \mid X$ .

#### 3.1 Proposed methodology

We propose instantiating the martingale posterior with the predictive rule induced by TabPFN through in-context learning. TabPFN is a *prior-data fitted network* (Müller et al., 2022), explicitly trained to approximate a Bayesian posterior predictive distribution (PPD) by sampling training data from exchangeable sequences defined by prior–likelihood pairs; see Appendix A for a review. We term the resulting martingale posterior **TabMGP**.

Several aspects of TabPFN directly support its role as a predictive rule in martingale posteriors:

1. In-context learning. At inference, TabPFN consumes both the observed context  $z_{1:i}$  and a new query  $x_{i+1}$ , and returns a one-step-ahead predictive distribution

$$P_i(\cdot \mid x_{i+1}) := \mathbb{P}(Y_{i+1} \in \cdot \mid x_{i+1}, z_{1:i}),$$

without retraining or fine-tuning. This property allows TabPFN to adapt to new datasets on the fly. We note that TabPFN can handles both classification and regression tasks: in classification it outputs a deterministic probability vector for  $y_{i+1}$ , while in regression it effectively performs multi-class classification by binning the response variable y.

- 2. Row-permutation invariance. Predictions in TabPFN depend only on the multiset  $\{z_1, \ldots, z_i\}$ , not on the order of its elements. This invariance is built into the TabPFN architecture, whereas many existing martingale posteriors (notably copula-based constructions, see Section 4) must enforce it by averaging predictive distributions over permutations of the feature order a process that is computationally expensive.
- 3. Bayesian alignment. As a prior-data fitted network, TabPFN is explicitly trained to approximate Bayesian posterior predictive distributions (PPDs). In the martingale posterior framework, the Bayesian PPD is in some sense the *ideal* predictive rule: if the predictive rule coincides with the true Bayesian PPD, then the resulting martingale posterior recovers the classical Bayesian posterior (see Appendix B). Training TabPFN on synthetic data generated from a wide range of prior–likelihood pairs encourages it to approximate this ideal behaviour across diverse tasks. This makes TabPFN's predictive distributions a more principled choice for constructing martingale posteriors.

Why not other transformers? Large language models and other pretrained transformers often exhibit in-context learning: given a context  $z_{1:i}$  and query  $x_{i+1}$ , they can produce a prediction for  $y_{i+1}$ . In this sense, they share the same basic mechanism as TabPFN. However, they lack the two further properties that make TabPFN especially well-suited as a predictive rule for martingale posteriors.

First, they are not row-permutation invariant. Because such models rely on positional embeddings, their predictions change with the ordering of training examples, unless explicit averaging is performed across permutations. Second, they are not trained to approximate Bayesian posterior predictive distributions: their training objectives are tailored to next-token prediction in text rather than calibrated probabilistic prediction for supervised tabular tasks. These differences mean that, although generic transformers can perform in-context learning, their predictive distributions are not naturally aligned with the martingale posterior framework. By contrast, TabPFN combines in-context learning with built-in permutation invariance and Bayesian alignment, making it a more principled choice.

### **Algorithm 1:** TabMGP

Validity of TabMGP as a martingale posterior. As noted in Section 2, we use the term "martingale posterior" in a broad sense: any predictive rule that induces a well-defined limiting distribution  $F_{\infty}$  gives rise to a posterior of the form (2), even if the rule does not satisfy the martingale or the almost conditionally identically distributed (a.c.i.d.) conditions (Battiston and Cappello, 2025), which are commonly used as sufficient guarantees. TabPFN does not meet these conditions (see Appendix C), but this does not preclude TabMGP from being a valid instance of the martingale posterior. Establishing more general criteria for the existence of  $F_{\infty}$  remains an open theoretical question. In the meantime, we assess validity empirically through diagnostics such as trace plots for the convergence of  $\theta(F_N)$  (Section 5) and concentration properties (Appendix C). Our empirical results indicate that TabMGP does converge and concentrate appropriately in practice.

Areas for improvement. TabMGP inherits several architectural limitations of TabPFN. One issue is that continuous responses are discretised through binning, effectively reducing regression to classification. While this enables TabPFN to reuse its classification machinery, it introduces approximation error that can distort uncertainty quantification. Another limitation is the lack of invariance to column permutations: predictions may depend on the arbitrary ordering of features, and TabPFN mitigates this by averaging over multiple random permutations at inference time. Although effective, a truly column-permutation-invariant architecture would be more principled and efficient. A further limitation concerns TabPFN's training objective: it optimises a final prediction loss rather than the autoregressive loss standard in transformer architectures. As a result, forward sampling requires repeated calls to the model, making TabMGP computationally heavy. If TabPFN were trained autoregressively, forward sampling could be implemented in a single network pass, greatly reducing cost.

#### 4 Related works

The martingale posterior framework admits many possible predictive rules, and a growing literature has explored different constructions. We review these constructions below, since they form the main competing methods for TabMGP in Section 5. In parallel, a separate line of work has asked whether the in-context learning behaviour of transformers satisfies martingale properties, which is especially relevant here since TabPFN is a transformer foundation model whose in-context learning defines our predictive rule.

Recent analyses (Falck et al., 2024; Ye and Namkoong, 2024; Nagler and Rügamer, 2025) show that the predictive rules induced by foundation models, such as TabPFN, are not martingales. Building on this line of work, we take the further step of testing the weaker a.c.i.d. condition (Battiston and Cappello, 2025) and show that TabPFN fails to satisfy it as well (Appendix C). Nevertheless, we find that the resulting TabMGP exhibits convergence (Appendix F) and near-nominal coverage (Section 5) in practice, suggesting that the usual sufficient conditions for validity are stricter than necessary.

Interestingly, Nagler and Rügamer (2025) adopt an approach closely aligned with ours, employing TabPFN as the predictive rule in the martingale posterior framework. Their finding that TabPFN is not a martingale leads them to abandon it as a predictive rule after the initial step, instead using its output to initialise a copula-based update that preserves martingale validity. By contrast, we retain TabPFN as the predictive rule throughout and interpret its failure to satisfy both the martingale and a.c.i.d. conditions as evidence that validity can be achieved under weaker assumptions.

We now give a brief summary of the main predictive rules developed in the martingale posterior literature.

**Bayesian boostrap** The Bayesian bootstrap (Rubin, 1981) is a predictive rule where future observations  $Z_{i+1}$  are uniformly drawn from the observations up to i:

$$Z_{i+1} \sim F_i, \quad i \ge n,$$

with  $F_i$  the empirical distribution of  $z_{1:i}$ . As this rule is discrete and unsmoothed, its use is recommended only when the functional of interest arises from a parametric likelihood loss, for which the smoothness of  $F_{\infty}$  is irrelevant (Fong et al., 2023; Dellaporta et al., 2022).

Newton's algorithm. Rooted in Bayesian nonparametrics, Newton's algorithm (Newton et al., 1998) was initially developed for unsupervised sequential learning in mixture models. It was subsequently reinterpreted as a predictive rule that generates a c.i.d. sequence of observations (Fortini and Petrone, 2020). This approach, however, is not suitable for high-dimensional  $\theta$ , as it requires numerical integration of an intractable normalising constant.

Copula-based updates. For applications requiring smoothness of  $F_{\infty}$ , the mainstream implementation of the martingale posterior is dominated by copula-based updates. Introduced by Hahn et al. (2018) and adopted as the default predictive rule in Fong et al. (2023), these updates smooth  $F_N$  by attaching a bivariate copula to each new observation while maintaining the martingale property on the predictive rule exactly. Subsequent work has extended this framework with autoregressive Gaussian-process likelihoods for higher-dimensional features (Ghalebikesabi et al., 2023), direct quantile updates (Fong and Yiu, 2024b), log-concave shape constraints (Cui and Walker, 2024), and vine copulas for very high dimensional features (Huk et al., 2024). All these variants preserve the exact martingale guarantee of the copula framework, but each introduces at least one smoothing or dependence hyperparameter, whose value controls the spread of the resulting martingale posterior.

Parametric plug-in predictives. For parametric inference, Walker (2022) and Holmes and Walker (2023) proposed a predictive rule of the form  $Z_{i+1} \sim p(\cdot \mid \widehat{\theta}_i)$ , where  $p(\cdot \mid \theta)$  is an assumed parametric model and  $\widehat{\theta}_i$  is a point estimate (e.g., maximum likelihood estimate) computed from all previous observations  $z_{1:i}$ . The asymptotic properties of this predictive rule are studied in Fong and Yiu (2024a). However, it requires that the assumed parametric model provides a reasonable approximation to the data distribution in order to yield sensible uncertainty quantification.

**Permutation-equivariant neural network.** Martingale posteriors have also been explored in the context of neural processes (Lee et al., 2023), where a permutation-equivariant neural network is used to construct a martingale posterior over latent variables. While this approach demonstrates the potential of using neural networks within a martingale posterior framework, the focus is still on prediction instead of inference, and it remains unclear how to generalize to broader statistical inference tasks.

### 5 Experiments

We compare TabMGP with other martingale posterior constructions using synthetic and real-world data. Our experiments focus on small- to moderate-n settings where the prior specification of the classical Bayesian posterior is important, making the martingale posterior particularly well suited.

To evaluate a given posterior  $\Pi(\cdot \mid z_{1:n})$ , we compute the *coverage* and 'size' of its joint  $(1 - \alpha)$  credible set  $C_{1-\alpha}(z_{1:n}) \subset \Theta$ :

$$\Pr_{\theta \sim \Pi(\cdot|z_{1:n})} (\theta \in C_{1-\alpha}(z_{1:n})) = 1 - \alpha.$$

Although the set can be constructed in different ways, an ellipsoidal approximation is often used for computational efficiency; see Appendix D for a discussion.

The coverage of  $C_{1-\alpha}(z_{1:n})$  is defined as

$$\Pr_{z_{1:n} \sim F_0} (\theta(F_0) \in C_{1-\alpha}(z_{1:n})), \tag{4}$$

namely, the proportion which the credible set contains the population risk minimiser,  $\theta(F_0) = \arg\min_{\theta} \int \ell(z,\theta) \, \mathrm{d}F_0(z)$ , under repeated draws of  $z_{1:n}$  from the true data-generating distribution  $F_0$ . Although frequentist in nature, this metric is commonly used for comparing Bayesian posteriors. We view higher coverage (closer to the nominal level), paired with a reasonably sized credible set, as indicative of more reliable and meaningful uncertainty quantification for the functional of interest.

**Posterior constructions.** We compare TabMGP against the martingale posteriors suggested in Fong et al. (2023): Bayesian bootstrap (BB) and the bivariate copula update (Copula). As a baseline, we also include the classical Bayesian posterior (Bayes) with an appropriate model and an isotropic Gaussian prior with variance 10<sup>2</sup>; the model choice is discussed later in this section when introducing the loss functions for this experiment. The exact computation details of the posteriors are provided in Appendix E.1.

**Loss functions.** We use negative log-likelihood as the loss in (1), and the corresponding model in the Bayes posterior. For continuous response (linear regression), we use  $\ell(x,y,\theta) = (y-[1\ x^{\top}]\theta)^2$  which is the negative log-likelihood of  $\mathcal{N}([1\ x^{\top}]\theta,1)$ . For K-class categorical response (logistic regression), we use  $\ell(x,y,\theta) = -\log \Pr(y=k)$ , where  $\Pr(y=k)$  is the k-th entry of the softmax applied to the logits  $([1\ x^{\top}]\theta_1,\ldots,[1\ x^{\top}]\theta_K)$ , and  $\theta_1,\ldots,\theta_K$  are the class-specific coefficients. We also set appropriate constraints on the coefficients to ensure identifiability in the loss function; see Appendix E.2 for details.

**Data-generating setups.** We describe the true data-generating distribution  $F_0$  of this experiment. For each  $F_0$ , we repeatedly sample 100 repetitions  $\{z_{1:n}^{(r)}\}_{r=1}^{100}$  from  $F_0$ . We refer to  $F_0$  together with the procedure used to generate  $z_{1:n}$  as a *setup*. The n is chosen to be as small as possible without rendering the design matrix ill-conditioned. In total, we have 30 setups (11 synthetic, 19 real-data) in this experiment.

Let  $\beta_0$  be a set of regression coefficients and  $x_i$  i.i.d. samples from a hypercube  $[-1,1]^{10}$ . For the synthetic setups, we generate  $y \mid x$  with:

- 1.  $y_i = x_i^{\top} \beta_0 + \epsilon_i$  where  $\epsilon_i \stackrel{iid}{\sim} \mathcal{N}(0,1)$ ;
- 2.  $y_i = x_i^{\top} \beta_0 + \epsilon_i$  where  $\epsilon_i$  are i.i.d. from  $t_5, \, t_4$  or  $t_3$ ;
- 3.  $y_i = x_i^{\top} \beta_0 + \epsilon_i$  where  $\epsilon_i$  is heteroscedastic and depends on  $x_i$ . We have three different strength of heteroscedasticity:  $s_1, s_2, s_3$ , from weak to strong;
- 4.  $y_i \mid x_i \stackrel{\text{iid}}{\sim} \text{Bernoulli}(L(x_i^{\top} \beta_0)), \text{ with a logistic link function } L;$
- 5.  $y_i \mid x_i \stackrel{\text{iid}}{\sim} \text{Bernoulli}(L(x_i^{\top}\beta_0))$ , where L is the distribution function of a Gaussian mixture model (GMM). We have models with three different location parameters: GMM(0), GMM(-1), GMM(-2).

For the 19 real-data setups, we use datasets from the OpenML and UCI repositories (9 continuous response, 8 binary response, and 2 multiclass categorical response). As  $F_0$  is unknown in the real-data setups, we take the empirical distribution of the entire dataset as the truth  $\tilde{F}_0$ . The details of all data-generating setups are given in Appendix E.3.

Metrics for comparing posteriors. For each posterior, we construct joint credible sets  $\widehat{C}_{1-\alpha}(z_{1:n})$  and compare their coverage (4) and 'size'. Our approach of constructing  $\widehat{C}_{1-\alpha}(z_{1:n})$  is described in Appendix E.4. We consider a posterior more reliable and meaningful when its credible set is small while achieving coverage at least at the the nominal level  $1-\alpha$ .

In the synthetic setups, the coverage is given by  $\frac{1}{100}\sum_{r=1}^{100}\mathbf{1}\big[\theta(F_0)\in\widehat{C}_{1-\alpha}(z_{1:n}^{(r)})\big]$ , where  $\{z_{1:n}^{(r)}\}_{r=1}^{100}$  are 100 replicates of  $z_{1:n}$  drawn from  $F_0$ . In the real-data setups, as  $F_0$  is unknown, we take the empirical distribution of the entire dataset  $\mathcal{D}$  as the truth  $\widetilde{F}_0$ , and compute the coverage on  $\theta(\widetilde{F}_0) = \arg\min_{\theta}\sum_{z\in\mathcal{D}}\ell(z,\theta)$ . That is, the coverage is  $\frac{1}{100}\sum_{r=1}^{100}\mathbf{1}\big[\theta(\widetilde{F}_0)\in\widehat{C}_{1-\alpha}(z_{1:n}^{(r)})\big]$ , where  $z_{1:n}^{(r)}$  denotes the r-th random draws (without replacement) from  $\mathcal{D}$ ; see Appendix E.3 for details. To quantify the 'size' of a credible set, we use the trace of the posterior covariance matrix as a proxy.

#### 5.1 Results

Convergence of  $\theta(F_N)$ . To conduct statistical inference, we require  $\theta(F_N)$  to converge  $\mathbb{P}$ -a.s. as  $N \to \infty$ . This convergence is commonly assessed via trace plots that track each dimension of  $\theta(F_N)$  as N increases, but this quickly becomes impractical for high-dimensional  $\theta$ . Instead, we track the expected  $L_1$ -norm of  $\theta(F_N)$  relative to the empirical risk minimiser  $\theta(F_n)$  as N increases; see Appendix F for the exact definition. We present the trajectories in Figure 1, where each trajectory corresponds to one of the 30 setups. This figure suggests that the trajectories (and hence  $\theta(F_N)$ ) generally converge as N increases, albeit with more noise in some setups.

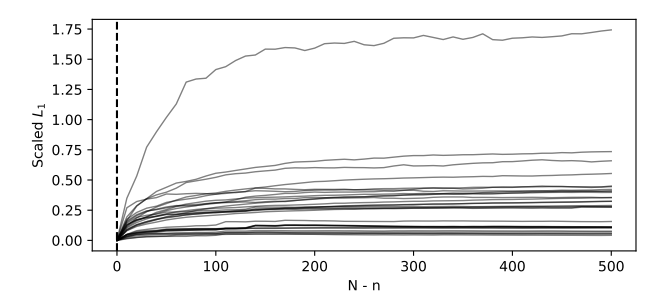


Figure 1: Expected  $L_1$ -norm between  $\theta(F_N)$  from TabMGP and  $\theta(F_n)$  as N increases. Each of the 30 trajectories corresponds to a realisation of  $z_{1:n}$  from one setup.

Shape of the posteriors. We present the marginals of the posteriors for a realisation of  $z_{1:n}$  in Figure 2 (intercept of 'concrete'), with the remaining dimension and setups provided in Appendix G. In general, the posterior means are similar across methods, but TabMGP often exhibits skewness and multimodal structure compared with the other posteriors, which are typically Gaussian-like. This suggests that TabMGP is more expressive than the other posteriors.

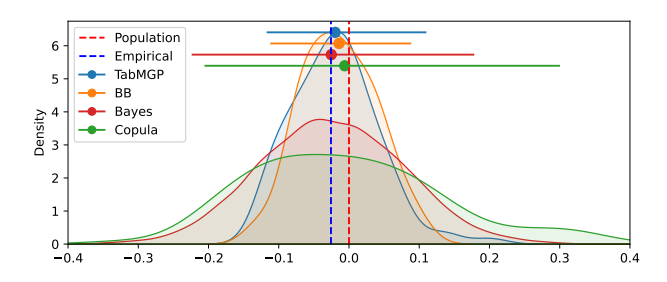


Figure 2: Posterior densities of the intercept in the 'concrete' setup. For each posterior density, the 95% marginal credible interval is shown as a horizontal bar, and the posterior mean as dots. The vertical dotted red and blue lines correspond to  $\theta(F_0)$  and  $\theta(F_n)$ , respectively.

**Joint credible sets of linear regression.** The results for synthetic data (top and middle) and real-data (bottom) setups are shown in Table 1. In the real-data setups, the rows are ordered by the n/p ratio in descending order, with  $p := \dim(\theta)$ .

TabMGP is competitive in both coverage and size (values in parentheses) of the credible set, performing particularly well on real data. Notably, it can attain almost 100% coverage in many setups while maintaining a small credible set. Similarly, Copula provides good coverage and small credible sets, although its sets are generally larger than those of TabMGP in most real-data setups. Bayes achieves close to 100% coverage in all setups, but its credible sets are much larger than those of TabMGP due to its diffuse prior. In contrast, BB tends to produce overly small sets with poor coverage in the synthetic setups (top and middle) and in low n/p settings (last few rows of Table 1). This reflects limited variability in forward samples when bootstrapping from a small  $z_{1:n}$  (e.g., n = 20 in the synthetic data setups).

$\overline{z_{1:n}}$	TabMGP	BB	Copula	Bayes
$\mathcal{N}(0,1)$	1.00 (0.45)	0.55(0.09)	0.99(0.35)	1.00 (1.29)
$t_5$	1.00(0.49)	0.65 (0.11)	0.99(0.37)	1.00(1.29)
$t_4$	0.99(0.51)	0.64 (0.12)	0.98(0.37)	1.00(1.30)
$t_3$	1.00(0.48)	0.66(0.14)	0.97  (0.35)	0.98 (1.30)
$\overline{s_1}$	1.00 (0.37)	0.50 (0.03)	1.00 (0.36)	1.00 (1.30)
$s_2$	1.00(0.36)	0.46 (0.02)	1.00(0.36)	1.00(1.30)
$s_3$	1.00(0.33)	0.53 (0.02)	1.00(0.37)	1.00(1.30)
concrete	0.91 (0.06)	0.80 (0.05)	1.00 (0.12)	1.00 (0.10)
quake	1.00(0.03)	0.95 (0.07)	1.00(0.18)	0.98(0.09)
airfoil	0.96(0.08)	0.93 (0.05)	0.97 (0.11)	1.00(0.12)
energy	1.00(0.04)	0.80 (0.01)	1.00(0.06)	1.00(0.14)
fish	0.90(0.10)	0.79(0.07)	0.95(0.10)	1.00(0.16)
kin8nm	0.95(0.13)	0.77 (0.09)	0.63 (0.08)	0.99(0.22)
auction	0.99(0.66)	0.86 (0.35)	0.97(1.44)	1.00(1.64)
grid	0.97(0.13)	0.72 (0.08)	0.88(0.10)	1.00(0.31)
abalone	0.97  (0.95)	0.66 (0.69)	0.94(0.98)	0.98(1.62)

Table 1: Experiments on linear regression: i.i.d. errors (top), dependent errors (middle), and real data (bottom). We compare TabMGP (ours), BB, Copula, and Bayes. Reported values are coverage and the trace of the posterior covariance (median, in parentheses), computed over 100 repetitions. Target coverage is 0.95.

Joint credible sets of logistic regression. The results for synthetic (top) and real-data (middle and bottom) setups are reported in Table 2. Copula was not applied to multinomial logistic regression (bottom) as the implementation of Fong et al. (2023) is not directly applicable. In the real-data setups, the rows are ordered by the n/p ratio in descending order within each section.

TabMGP generally yields the smallest credible sets with good coverage (typically above 95%), except in the synthetic setups, where it slightly under-covers. Bayes is the next best, attaining nearly 100% coverage and producing credible sets that are generally smaller than those of BB and Copula, but larger than those of TabMGP. BB performs reasonably well in binary logistic regression (top and middle), although its credible sets are larger than those of TabMGP. However, BB severely under-covers in multinomial logistic regression (bottom), where p is much greater than in the other logistic regression setups. Copula performs poorly in logistic regression, producing trivial credible sets. This indicates that Copula is sensitive to the choice of bandwidth, as the same value yields good performance in the linear regression experiment.

Marginal credible intervals. In addition to the results of joint credible sets presented above, we also report the results of marginal credible intervals in Appendix H. We report both the coverage and the Winkler score (Winkler, 1972), a widely used scoring rule for assessing univariate interval estimates. By this metric,

$\overline{z_{1:n}}$	TabMGP	BB	Copula	Bayes
Logistic	0.84 (1.30)	0.83 (1.96)	1.00 (2.72)	0.99 (1.94)
GMM(0)	0.91(2.44)	0.91(4.14)	1.00(4.01)	0.99(3.66)
GMM(-1)	0.83 (1.27)	0.86 (1.95)	1.00(2.64)	1.00(1.95)
GMM(-2)	0.78  (0.88)	0.78(1.36)	1.00(2.08)	1.00(1.37)
rice	1.00 (3.74)	0.88 (7.35)	1.00 (28.4)	1.00 (6.66)
sepsis	0.95(0.69)	1.00(2.42)	1.00 (10.0)	1.00(3.23)
banknote	0.99(1.16)	1.00(1.48)	1.00(1.53)	1.00(1.48)
mozilla	0.96 (1.42)	0.97(2.04)	1.00(2.68)	0.96(1.42)
skin	1.00(1.39)	1.00(1.84)	1.00(1.80)	1.00(1.49)
blood	0.87 (1.07)	0.95 (2.51)	1.00(5.40)	1.00(2.06)
phoneme	1.00(1.32)	0.95 (1.92)	1.00(5.62)	1.00(2.15)
telescope	0.99(5.96)	0.99(10.7)	1.00(50.7)	1.00(9.39)
yeast	0.97 (11.1)	0.68 (25.1)		1.00 (26.9)
wine	0.93 (11.0)	0.79 (39.7)		0.98(33.1)

Table 2: Experiments on logistic regression: synthetic data with various link functions (top), real data with binary logistic regression (middle), and real data with multinomial logistic regression (bottom). We compare TabMGP (ours), BB, Copula, and Bayes. Reported values are coverage and the trace of the posterior covariance (median, in parentheses), computed over 100 repetitions. Target coverage is 0.95.

TabMGP tends to perform better for logistic regression, whereas BB performs better for linear regression despite being severely under-covered most of the time. Across the 293 regression coefficients considered, TabMGP is preferred 155 times, BB 125 times, Copula 11 times, and Bayes 2 times.

Computation time. The main computational cost of martingale posteriors is forward sampling, which is readily parallelisable. Per sample, BB is fastest (near-instantaneous); Copula takes 10–20s; and TabMGP takes about 70s (binary/categorical response) or 200s (continuous response). The NUTS algorithm (Bayes) runs in under 60s. BB, Copula, and Bayes are implemented in compiled JAX, whereas TabMGP currently runs in uncompiled PyTorch. We expect this gap to narrow with further code optimisation. All experiments were conducted on an Nvidia L40s.

### 6 Conclusion

We introduced TabMGP, a new construction of the martingale posterior that uses a pre-trained tabular foundation model, TabPFN, as its predictive rule. This approach circumvents the usual challenges of prior specification in classical Bayesian inference and the need to design bespoke predictive rules in existing martingale posterior frameworks. By utilising the in-context learning capabilities of transformers, TabMGP provides an off-the-shelf tool for statistical inference. Across a wide range of synthetic and real-world datasets, our empirical evaluation shows that TabMGP delivers reliable uncertainty quantification.

Our findings also expose limitations in the current theoretical understanding of martingale posteriors. Existing analyses emphasise sufficient conditions such as the martingale or a.c.i.d. properties, yet TabPFN fails both while still yielding posteriors that converge and achieve near-nominal coverage in practice. This suggests that the present theory is overly restrictive and does not yet capture the range of predictive rules that work well empirically. Developing weaker and more realistic conditions is an important direction for future research, particularly as martingale posteriors are likely to be combined with an increasing variety of black-box predictive models. Strengthening the theoretical foundations of this marriage will be crucial for ensuring that such methods can be used with confidence in practice.

Beyond its role in the post-Bayes expansion, our perspective is also potentially relevant for deep learning interpretability. A pretrained transformer, when used through in-context learning, implicitly defines a pre-

dictive rule. The Bayesian predictive framework raises the intriguing possibility that if this rule induces asymptotic exchangeability, then de Finetti's representation theorem applies and the transformer can be viewed as carrying a hidden prior–likelihood pair (Fortini and Petrone, 2025). Thus the Bayesian predictive framework could provide a new lens on the internal structure of foundation models.

### Acknowledgments

The authors would like to thank Abdelhamid Ezzerg, Joshua Bon, Christian Robert, Lorenzo Cappello, Jack Jewson, Rubén Loaiza-Maya and Anastasios Panagiotelis for helpful comments in the development of this work. KN was supported by the Australian Government Research Training Program and the Statistical Society of Australia PhD Top-up Scholarship. EF was supported by the Research Grants Council of Hong Kong through the General Research Fund (17307321) and the Early Career Scheme (27304424). DTF acknowledges funding from the Australian Research Council (DE200101070, DP200101414). JK was supported through the UK's Engineering and Physical Sciences Research Council (EPSRC) via EP/W005859/1. SW was supported by the Australian Research Council (DE200101253). Computational resources were provided by the ARDC Nectar Research Cloud.

### References

- Aitchison, J. (1975). Goodness of prediction fit, Biometrika 62(3): 547-554.
- Battiston, M. and Cappello, L. (2025). New (and old) predictive schemes with a.c.i.d. sequences. arXiv:2507.21874.
- Berti, P., Dreassi, E., Pratelli, L. and Rigo, P. (2021). A class of models for Bayesian predictive inference, Bernoulli 27(1): 702–726.
- Berti, P., Pratelli, L. and Rigo, P. (2004). Limit theorems for a class of identically distributed random variables, *The Annals of Probability* **32**(3): 2029–2052.
- Bissiri, P. G., Holmes, C. C. and Walker, S. G. (2016). A general framework for updating belief distributions, Journal of the Royal Statistical Society: Series B (Statistical Methodology) 78(5): 1103–1130.
- Bommasani, R., Hudson, D. A., Adeli, E., Altman, R., Arora, S., von Arx, S., Bernstein, M. S., Bohg, J., Bosselut, A., Brunskill, E., Brynjolfsson, E., Buch, S., Card, D., Castellon, R., Chatterji, N., Chen, A., Creel, K., Davis, J. Q., Demszky, D., Donahue, C., Doumbouya, M., Durmus, E., Ermon, S., Etchemendy, J., Ethayarajh, K., Fei-Fei, L., Finn, C., Gale, T., Gillespie, L., Goel, K., Goodman, N., Grossman, S., Guha, N., Hashimoto, T., Henderson, P., Hewitt, J., Ho, D. E., Hong, J., Hsu, K., Huang, J., Icard, T., Jain, S., Jurafsky, D., Kalluri, P., Karamcheti, S., Keeling, G., Khani, F., Khattab, O., Koh, P. W., Krass, M., Krishna, R., Kuditipudi, R., Kumar, A., Ladhak, F., Lee, M., Lee, T., Leskovec, J., Levent, I., Li, X. L., Li, X., Ma, T., Malik, A., Manning, C. D., Mirchandani, S., Mitchell, E., Munyikwa, Z., Nair, S., Narayan, A., Narayanan, D., Newman, B., Nie, A., Niebles, J. C., Nilforoshan, H., Nyarko, J., Ogut, G., Orr, L., Papadimitriou, I., Park, J. S., Piech, C., Portelance, E., Potts, C., Raghunathan, A., Reich, R., Ren, H., Rong, F., Roohani, Y., Ruiz, C., Ryan, J., Ré, C., Sadigh, D., Sagawa, S., Santhanam, K., Shih, A., Srinivasan, K., Tamkin, A., Taori, R., Thomas, A. W., Tramèr, F., Wang, R. E., Wang, W., Wu, B., Wu, J., Wu, Y., Xie, S. M., Yasunaga, M., You, J., Zaharia, M., Zhang, M., Zhang, T., Zhang, X., Zhang, Y., Zheng, L., Zhou, K. and Liang, P. (2022). On the Opportunities and Risks of Foundation Models. arXiv:2108.07258.
- Cui, F. and Walker, S. G. (2024). Martingale posterior distributions for log-concave density functions. arXiv:2401.14515.
- Dellaporta, C., Knoblauch, J., Damoulas, T. and Briol, F.-X. (2022). Robust Bayesian inference for simulator-based models via the MMD posterior bootstrap, *Proceedings of the International Conference on Artificial Intelligence and Statistics*, pp. 943–970.
- Doob, J. L. (1949). Application of the theory of martingales, Le Calcul des Probabilites et ses Applications pp. 23–27.

- Falck, F., Wang, Z. and Holmes, C. (2024). Is in-context learning in large language models Bayesian? A martingale perspective, *Proceedings of the International Conference on Machine Learning*.
- Fong, E., Holmes, C. and Walker, S. G. (2023). Martingale posterior distributions, *Journal of the Royal Statistical Society: Series B (Statistical Methodology)* 85(5): 1357–1391.
- Fong, E. and Yiu, A. (2024a). Asymptotics for parametric martingale posteriors. arXiv:2410.17692.
- Fong, E. and Yiu, A. (2024b). Bayesian quantile estimation and regression with martingale posteriors. arXiv:2406.03358.
- Fortini, S. and Petrone, S. (2020). Quasi-Bayes properties of a procedure for sequential learning in mixture models, *Journal of the Royal Statistical Society: Series B (Statistical Methodology)* 82(4): 1087–1114.
- Fortini, S. and Petrone, S. (2025). Exchangeability, prediction and predictive modeling in Bayesian statistics, Statistical Science 40(1): 40–67.
- Ghalebikesabi, S., Holmes, C. C., Fong, E. and Lehmann, B. (2023). Quasi-Bayesian nonparametric density estimation via autoregressive predictive updates, *Proceedings of the Conference on Uncertainty in Artificial Intelligence*, pp. 658–668.
- Hahn, P. R., Martin, R. and Walker, S. G. (2018). On recursive Bayesian predictive distributions, *Journal of the American Statistical Association* **113**(523): 1085–1093.
- Hoffman, M. D. and Gelman, A. (2014). The No-U-turn sampler: Adaptively setting path lengths in Hamiltonian Monte Carlo., *Journal of Machine Learning Research* **15**(1): 1593–1623.
- Hollmann, N., Müller, S., Eggensperger, K. and Hutter, F. (2022). TabPFN: A transformer that solves small tabular classification problems in a second, *NeurIPS 2022 First Table Representation Workshop*.
- Hollmann, N., Müller, S., Purucker, L., Krishnakumar, A., Körfer, M., Hoo, S. B., Schirrmeister, R. T. and Hutter, F. (2025). Accurate predictions on small data with a tabular foundation model, *Nature* **637**(8045): 319–326.
- Holmes, C. C. and Walker, S. G. (2023). Statistical inference with exchangeability and martingales, *Philosophical Transactions of the Royal Society A: Mathematical, Physical and Engineering Sciences* **381**(2247): 20220143.
- Huk, D., Zhang, Y., Dutta, R. and Steel, M. (2024). Quasi-Bayes meets Vines, Advances in Neural Information Processing Systems.
- Hyndman, R. J. (1996). Computing and graphing highest density regions, *The American Statistician* **50**(2): 120–126.
- Knoblauch, J., Jewson, J. and Damoulas, T. (2022). An optimization-centric view on Bayes' rule: Reviewing and generalizing variational inference, *Journal of Machine Learning Research* **23**(132): 1–109.
- Lee, H., Yun, E., Nam, G., Fong, E. and Lee, J. (2023). Martingale posterior neural processes, *International Conference on Learning Representations*.
- Müller, S., Hollmann, N., Arango, S. P., Grabocka, J. and Hutter, F. (2022). Transformers can do Bayesian inference, *International Conference on Learning Representations*.
- Nagler, T. and Rügamer, D. (2025). Uncertainty quantification for prior-data fitted networks using martingale posteriors. arXiv:2505.11325.
- Newton, M. A., Quintana, F. A. and Zhang, Y. (1998). Nonparametric Bayes methods using predictive updating, *Practical Nonparametric and Semiparametric Bayesian Statistics*, Springer, New York, NY, pp. 45–61.

- Pedregosa, F., Varoquaux, G., Gramfort, A., Michel, V., Thirion, B., Grisel, O., Blondel, M., Prettenhofer, P., Weiss, R., Dubourg, V., Vanderplas, J., Passos, A., Cournapeau, D., Brucher, M., Perrot, M. and Duchesnay, É. (2011). Scikit-learn: Machine learning in Python, *Journal of Machine Learning Research* 12(85): 2825–2830.
- Rubin, D. B. (1981). The Bayesian bootstrap, The Annals of Statistics 9(1): 130–134.
- Shen, Z., Knoblauch, J., Power, S. and Oates, C. J. (2025). Prediction-centric uncertainty quantification via MMD, *Proceedings of the International Conference on Artificial Intelligence and Statistics*, pp. 649–657.
- Walker, S. G. (2022). Chapter 4 A new look at Bayesian uncertainty, *Handbook of Statistics*, Vol. 47 of *Advancements in Bayesian Methods and Implementation*, Elsevier, pp. 83–101.
- Wild, V. D., Ghalebikesabi, S., Sejdinovic, D. and Knoblauch, J. (2023). A rigorous link between deep ensembles and (variational) Bayesian methods, *Advances in Neural Information Processing Systems*.
- Winkler, R. L. (1972). A decision-theoretic approach to interval estimation, *Journal of the American Statistical Association* **67**(337): 187–191.
- Wu, P.-S. and Martin, R. (2023). A comparison of learning rate selection methods in generalized Bayesian inference, Bayesian Analysis 18(1): 105–132.
- Ye, N. and Namkoong, H. (2024). Exchangeable sequence models quantify uncertainty over latent concepts. arXiv:2408.03307.
- Zhang, Y. D., Naughton, B. P., Bondell, H. D. and Reich, B. J. (2022). Bayesian regression using a prior on the model fit: The R2-D2 shrinkage prior, *Journal of the American Statistical Association* **117**(538): 862–874.

#### A Review of TabPFN

A precursor to TabPFN can be found in Müller et al. (2022), where the transformer is simply called a priordata-fitted network (PFN). The premise is predicated that shows the Bayes posterior predictive density is optimal in an *average* sense. We present this in the unsupervised setting to keep the notation lightweight on a result<sup>1</sup> in Aitchison (1975).

Suppose we have an exchangeable distribution

$$p(z_1, ..., z_n) = \int \prod_{i=1}^n p(z_i \mid \nu) \phi(\nu) \, d\nu.$$
 (5)

Consider the Kullback-Leibler (KL) divergence between  $p(z \mid \nu)$  and some predictive density  $q(z \mid z_{1:n})$  where  $z_{1:n}$  is drawn from (5), i.e., first draw  $\nu$  from the prior  $\phi(\nu)$  and then draw  $z_i$  i.i.d. from  $p(z \mid \nu)$ . Then,

$$D_{\mathrm{KL}}(p(z \mid \nu) || q(z \mid z_{1:n}))$$

is random because a)  $\nu$  is random and b) the data  $z_{1:n}$  is random. By integrating out these sources of randomness, we get an average KL divergence, a deterministic quantity

$$\mathbb{E}_{\nu, z_{1:n}} D_{\mathrm{KL}}(p(z \mid \nu) \parallel q(z \mid z_{1:n})) = \int \phi(\nu) \, \mathrm{d}\nu \int p(z_{1:n} \mid \nu) \, \mathrm{d}z_{1:n} \int p(z \mid \nu) \log \frac{p(z \mid \nu)}{q(z \mid z_{1:n})} \, \mathrm{d}z.$$
 (6)

Aitchison (1975) then shows that the predictive density q that minimizes this average KL divergence in (6) is none other than the Bayesian posterior predictive density (PPD) corresponding to the likelihood-prior pair in (5):

$$p(z \mid z_{1:n}) = \int p(z \mid \nu) \pi(\nu \mid z_{1:n}) \, d\nu$$
 (7)

 $<sup>^{1}</sup>$ Though the work Müller et al. (2022) does not appear to be aware of this result

where  $\pi(\nu \mid z_{1:n}) \propto \prod_{i=1}^{n} p(z_i \mid \nu) \phi(\nu)$ , the standard Bayesian posterior construction.

This optimality result for the Bayesian PPD immediately suggests a meta-learning training objective. Since minimising the average KL divergence with respect to q is indifferent to the entropy term of  $p(z \mid \nu)$  in the KL divergence, we may rewrite the objective as

$$\underset{q(z \mid z_{1:n})}{\arg\min} \, E_{\nu, z_{1:n}} \, \mathrm{KL}(p(z \mid \nu) \, \| \, q(z \mid z_{1:n})) = \underset{q(z \mid z_{1:n})}{\arg\min} \, E_{\nu, z_{1:n}} \, E_{p(z \mid \nu)} - \log q(z \mid z_{1:n})$$

to which the empirical risk counterpart is

$$\underset{w}{\operatorname{arg\,min}} - \sum_{m=1}^{M} \sum_{k=1}^{K} \log q_{w}(z_{n+k}^{m} \mid z_{1:n}^{m}).$$

if we use a model  $q_w$ . Here,  $q_w$  can be any model that can accept a variable length set  $z_{1:n}$  and returns a distribution over future z, and the samples  $z_{1:n+K}$  are drawn from an exchangeable distribution  $p(z_1, \ldots, z_n, z_{n+1}, \ldots, z_{n+K})$  as in (5). Müller et al. (2022) choose to use a variant of transformers for  $q_w$ . This is most natural when z is categorical. In the case of real-valued z, Müller et al. (2022) perform an adaptive binning operation that essentially converts the regression to a classification task.

Later developments led to the TabPFN Hollmann et al. (2022; 2025) which trains on a vast amount of synthetic data generated from a very large array of likelihood-prior pairs, rather than a single pair as in the original PFN work. This gives TabPFN the qualifier foundational.

# B Recovering classical Bayesian posterior from martingale posterior.

A sample from the classical Bayesian posterior  $\pi(\theta \mid z_{1:n}) \propto \pi(\theta) \prod_{i=1}^{n} p(z_i \mid \theta)$  can be equivalently obtained from the martingale posterior. This is achieved by forward sampling with Bayesian PPD:

$$p(z \mid z_{1:i}) = \int p(z \mid \theta) \, \pi(\theta \mid z_{1:i}) \, \mathrm{d}\theta,$$

then compute the posterior mean estimator  $\mathbb{E}[\theta \mid z_{1:\infty}]$ . This is a result from the Doob's martingale convergence theorem (Doob, 1949). Alternatively, we can use the maximum likelihood estimator as our functional of interest  $\theta(F)$ , i.e., setting the loss in (1) as  $\ell(z,\theta) = -\log p(z \mid \theta)$ , and the distribution of  $\theta(F_{\infty})$  will be  $\pi(\theta \mid z_{1:n})$ . This is due to the asymptotic equivalence of a posterior mean estimator and the maximum likelihood estimator.

# C Validity of TabMGP as a martingale posterior.

As discussed in Section 2, a sufficient condition for the existence of  $F_{\infty}$  and hence for the martingale posterior distribution to be well-defined, is that the sequence  $(P_i)_{i\geq 0}$  is a martingale, or equivalently, that the sequence  $(Z_i)_{i\geq 1}$  is conditionally identically distributed (c.i.d, Berti et al., 2004). The martingale property stipulates that  $(P_i)_{i\geq 0}$  satisfies, for every  $i\geq 0$  and every measurable set A:

$$\mathbb{E}(P_{i+1}(A) \mid Z_{1:i}) = P_i(A). \tag{8}$$

A relaxations of this sufficient condition is the almost conditionally identically distributed (a.c.i.d.) condition (Battiston and Cappello, 2025). Let  $(\xi_i)_{i\geq 1}$  be a sequence of non-negative random variables. The sequence  $(Z_i)_{i\geq 1}$  is a.c.i.d. if the corresponding predictive rule  $(P_i)_{i\geq 0}$  satisfies

$$|\mathbb{E}_{Z_{i+1}}(P_{i+1}(A) \mid Z_{1:i}) - P_i(A)| \le \xi_i, \quad \text{a.s.},$$
(9)

for all  $i \geq 1$  and all measurable sets A. Battiston and Cappello (2025) show that  $F_{\infty}$  exists if  $\sum_{i=0}^{\infty} \xi_i < \infty$ ,  $\mathbb{P}$ -a.s., and that the sequence  $(Z_i)_{i\geq 1}$  is  $F_{\infty}$ -asymptotically exchangeable. We will refer to these conditions collectively as the a.c.i.d. condition. Clearly, (9) generalises the stronger martingale condition (8), i.e.,  $\xi_i = 0$  for all  $i \geq 1$ , and we will use (9) to verify the existence of  $F_{\infty}$  for TabMGP instead of (8).

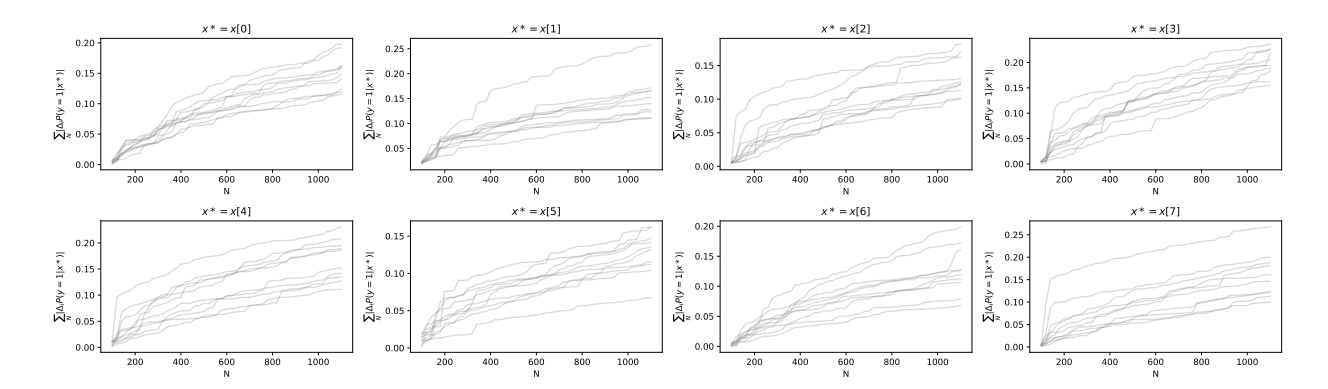


Figure 3: Cumulative sum (over N) of the  $L_1$ -distance between  $\mathbb{E}_{y_{i+1}}[p_{i+1}(y \mid x^*) \mid z_{1:i}]$  and  $p_i(y \mid x^*)$  across eight choices of  $x^*$ . Ideally, this cumulative sum converges to satisfy the a.c.i.d. condition.

Verifying (9) empirically is generally challenging, as it must hold for all measurable sets A. Rather, we adopt an equivalent formulation in terms of total variation distance (Battiston and Cappello, 2025):

$$\sum_{i=1}^{\infty} \text{TV}\left(\mathbb{E}_{Z_{i+1}}(P_{i+1}(\cdot) \mid Z_{1:i}), P_i(\cdot)\right) \leq \xi_i, \quad \text{a.s.},$$

for all  $i \ge 0$ . Since the predictive distributions of both TabPFN and the Bayesian bootstrap are probability mass functions  $p_i$ , the condition can be further simplified in terms of the  $L_1$  distance:

$$\sum_{i=1}^{\infty} \sum_{z \in \mathcal{Z}} |\mathbb{E}_{Z_{i+1}}[p_{i+1}(z) \mid Z_{1:i}] - p_i(z)| < \infty, \quad \text{a.s..}$$
 (10)

There are several practical considerations when estimating (10). First, we start the outer summation from i = n, as TabPFN requires a small number of initial observations to produce reliable predictions. Second, in our supervised learning setting where z = (x, y), the expectation

$$\mathbb{E}_{Z_{i+1}}[p_{i+1}(z) \mid z_{1:i}] = \mathbb{E}_{Y_{i+1}, X_{i+1}}[p_{i+1}(y \mid x_{i+2}) p_{i+1}(x) \mid z_{1:i}],$$

requires a large number of Monte Carlo samples and is computationally demanding. To mitigate this, we fix all future covariates  $x_{n+1:N+2}$  to a constant value  $x^*$  and consider the weaker condition:

$$\sum_{i=n}^{N} \sum_{y \in \mathcal{Y}} |\mathbb{E}_{Y_{i+1}}[p_{i+1}(y \mid x^{\star}) \mid z_{1:i}] - p_i(y \mid x^{\star})| < \infty, \tag{11}$$

for a sufficiently large N. We then compute (11) repeatedly over many realisations of  $Y_{n+1:N}$ .

We evaluate this condition on a dataset generated as  $y_i \stackrel{i.i.d.}{\sim} \text{Bernoulli}(\text{logistic}(x_i^{\top}\beta_0))$ , for  $i=1,\ldots,100$ , with some fixed  $\beta_0 \in \mathbb{R}^2$ . Our empirical results (Figure 3) indicate that the predictive rule induced by TabPFN does not strictly satisfy the a.c.i.d. condition. This negative result, however, does not imply non-convergence to  $F_{\infty}$  for TabMGP, as the a.c.i.d. condition is only sufficient, not necessary.

As an alternative, we track the sample path of  $\theta(F_N)$  as N increases, as in Fong et al. (2023). After all, we need  $\theta(F_N)$  to converge  $\mathbb{P}$ -a.s. to conduct meaningful statistical inference. We refer to these diagnostic plots as the "trace plot" and inspect them in Appendix F. We observe that the sample path of  $\theta(F_N)$  does converge in most of our experiment, thus suggesting that the a.c.i.d. condition is too restrictive for our purpose of establishing the existence of  $\theta(F_\infty)$ .

For completeness, we further demonstrate that TabMGP can concentrate close to  $\theta_0$  as the sample size n grows. To illustrate this, we use a regression dataset, since the sum of the sample size needed for meaningful

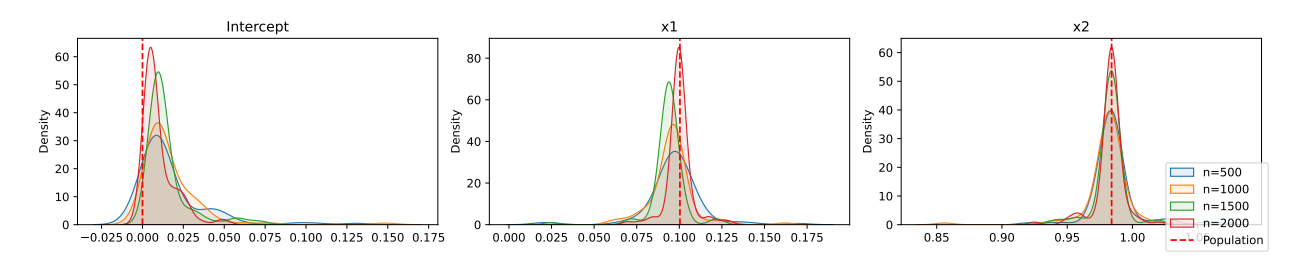


Figure 4: Concentration of TabMGP. The red vertical line indicates the population risk minimiser  $(0, \beta_0^{\perp})$ .

concentration and the forward sampling steps required for convergence in classification exceeds TabPFN's 10,000-context length limit. The regression dataset is defined as  $y_i \overset{i.i.d.}{\sim} \mathcal{N}(x_i^{\top}\beta_0, 0.1^2)$ ,  $i = 1, \ldots, n$ , for some fixed  $\beta_0 \in \mathbb{R}^2$ , with the loss function  $\ell(x, y, \theta) = (y - [1 \ x^{\top}]\theta)^2$ . Ideally, TabMGP should concentrate on  $\theta_0 = [0, \beta_0^{\top}]$  as n increases. Figure 4 confirms that TabMGP indeed concentrates around  $\theta_0$ .

## D Highest-posterior density credible sets

The highest-posterior-density (HPD) credible set is a common construction of a Bayesian credible set. The HPD set at level  $1 - \alpha$  is defined as

$$C_{1-\alpha}^{\text{HPD}} = \left\{ \theta \in \mathbb{R}^p : \pi(\theta \mid z_{1:n}) \ge t_{1-\alpha} \right\},\,$$

where  $t_{1-\alpha}$  is chosen such that  $\int_{C_{1-\alpha}^{\text{HPD}}} \pi(\theta \mid z_{1:n}) d\theta = 1 - \alpha$ . By construction,  $C_{1-\alpha}^{\text{HPD}}$  has minimum volume among all sets of posterior probability  $1-\alpha$ , making it the "gold standard" for summarising joint uncertainty (Hyndman, 1996).

In many models — particularly linear and logistic regressions with well-behaved posteriors — the posterior is approximately multivariate normal:

$$\theta \mid z_{1:n} \approx \mathcal{N}_p(\hat{\mu}, \hat{\Sigma}).$$

In these cases, the HPD set reduces to the  $\chi^2$ -ellipsoid

$$C_{1-\alpha}^{\text{HPD}} \approx \left\{ \theta : (\theta - \hat{\mu})^{\top} \hat{\Sigma}^{-1} (\theta - \hat{\mu}) \le \chi_{p,1-\alpha}^2 \right\}, \tag{12}$$

treating the Mahalanobis ellipsoid as the HPD set under the normal approximation.

## **E** Experimental settings and hyperparameters

The code is released at https://anonymous.4open.science/r/tabmgp-366A.

#### E.1 Posterior constructions

**Settings of Bayes.** We approximate the posterior using a No-U-turn sampler (NUTS, Hoffman and Gelman, 2014) with 1000 warm-up steps, followed by 2000 sampling steps across 4 chains with different initialisations, for a total of 8000 samples.

Settings for all martingale posteriors. We run 2000 forward-sampling steps for both BB and Copula. For TabMGP, we find that N = n + 500 is sufficient for  $\theta(F_N)$  to converge (Figure 1 and Appendix F) and use only 500 forward-sampling steps. We approximate all martingale posterior constructions with 100 samples.

Settings of TabMGP. The logits of the predictive rules are obtained from TabPFNClassifier.predict\_proba for logistic regression and TabPFNRegressor.predict(output\_type = "full") for linear regression. By default, these logits are scale by a temperature of 0.9. For our experiments, we use the untempered logits as our predictive rules, i.e., setting the temperature to 1. By construction, TabPFN is not permutation invariant to the order of the dimensions of labels y and features x. The default implementation of TabPFN uses an ensemble of predictions from randomly permuting the dimensions of labels and features. The resulting probability mass functions are then averaged to get the final predictive mass function. We use the default number of ensemble in version 2.0.6, which is 4 for classifiers and 8 for regressors.

We use the following two checkpoints:

- Classifier: https://huggingface.co/Prior-Labs/TabPFN-v2-clf/blob/main/tabpfn-v2-classifier.ckpt
- Regressor: https://huggingface.co/Prior-Labs/TabPFN-v2-reg/blob/main/tabpfn-v2-regressor.ckpt

These are the default checkpoints at the time of running our experiments, and the transformer was pre-trained exclusively on synthetic, exchangable sequence of data. Subsequent iterations of the TabPFN checkpoints, however, have been fine-tuned on real-world datasets, and these checkpoints are not used in our experiments.

**Settings of Copula.** We use the copula construction in Fong et al. (2023, §4.4.2 and §4.4.3) with the bandwidth fixed to 0.8, since for our experiments the marginal-likelihood-based tuning procedure of Fong et al. (2023) produces values that are too small and delivers poor results. Instead, we estimate

$$\theta(P_N) \approx \underset{\theta}{\operatorname{arg\,min}} \sum_i \ell(\widetilde{x}_i, \widetilde{y}_i, \theta),$$

where  $(\widetilde{x}_i, \widetilde{y}_i)_{i \geq 0}$  are generated by iterating  $\widetilde{x}_i$  over  $x_{1:n}$  and, for each  $\widetilde{x}_i$ , drawing  $\widetilde{y}_i$  from  $P_N(\cdot \mid \widetilde{x}_i)$ . We repeat this procedure five times, yielding 5n pairs of  $(\widetilde{x}_i, \widetilde{y}_i)$ .

#### E.2 Specification of the loss function

We set the following coefficients to 0 to ensure identifiablity in the loss function:

- 1. The coefficients for the first level of each categorical feature;
- 2. The coefficients corresponding to all (almost) collinear features;
- 3. In logistic regression, the coefficients corresponding to the first category,  $\theta_1$ .

We identify the collinear features as those with the largest loading in the least important principal component of the population data, removing them one at a time until the computation of  $\theta(F_0)$  is numerically stable. The resulting parameter dimension,  $p := \dim(\theta)$ , and the features used in the functional are listed in Table 3 and Table 4, respectively.

We then standardise all continuous response and features using the population mean and variance, and one-hot encode all categorical features. Using population moments for standardisation ensures that  $\theta$  remains on a common scale across repetitions.

#### E.3 Data setups

**Synthetic data.** The 11 synthetic setups are adapted from Wu and Martin (2023, Section 5): the features  $x_i$  are i.i.d. and uniformly sampled from the hypercube  $[-1,1]^{10}$ . The true coefficients  $\beta_0$  are sampled once from  $[-2,3]^{10}$  and held fixed across the 100 repetition of  $z_{1:n}$ . The response  $y \mid x$  is generated as follows:

- Continuous i.i.d. response (4 setups): We generate n = 20 samples from  $y_i = x_i^{\top} \beta_0 + \epsilon_i$ , i = 1, ..., n. The errors  $\epsilon_i$  are either i.i.d.  $\mathcal{N}(0, 1)$  or Student-t with 5, 4, or 3 degrees of freedom. Note that  $\theta(F_0)$  coincides with  $(0, \beta_0^{\top})$  in the case of i.i.d. N(0, 1) error.
- Continuous response with heteroscedastic errors (3 setups): We generate n=20 samples from  $y_i=x_i^{\top}\beta_0+\epsilon_i, i=1,\ldots,n$ , where  $\epsilon_i\sim\mathcal{N}(0,\sigma_i^2)$ . The standard deviation of the error  $\sigma_i$  is determined by the first coordinate of  $x_i$ :

$$\sigma_i = \begin{cases} s_{\text{left}}, & \text{if } x_{i1} < \hat{\xi}_{0.25}, \\ s_{\text{mid}}, & \text{if } \hat{\xi}_{0.25} \le x_{i1} \le \hat{\xi}_{0.75}, \\ 1, & \text{if } x_{i1} > \hat{\xi}_{0.75}, \end{cases}$$

where  $\hat{\xi}_{0.25}$  and  $\hat{\xi}_{0.75}$  are the empirical quartiles of  $x_{11}, \ldots, x_{n1}$ . The hyperparameters  $(s_{\text{left}}, s_{\text{mid}})$  are arranged by their deviation from  $\sigma = 1$ , ranging from weak to strong:  $s_1 = (0.25, 0.5)$ ,  $s_2 = (0.05, 0.25)$ , and  $s_3 = (0.01, 0.1)$ .

• Binary response (4 setups): We generate n = 100 samples from  $y_i \mid x_i \stackrel{\text{iid}}{\sim} \text{Bernoulli}(L(x_i^{\top}\beta_0)), i = 1, \ldots, n$ , with different link functions L. The link is either the logistic function:

$$L(u) = (1 + \exp(-u))^{-1},$$

or the distribution function of a Gaussian-mixture model (GMM):

$$L(u) = 0.7 \Phi(u \mid a, 1) + 0.3 \Phi(u \mid 2, 1),$$

where  $\Phi(\cdot \mid m, 1)$  denotes the distribution function of a Gaussian with mean m and unit variance, and  $a \in \{0, -1, -2\}$ . Note that  $\theta(F_0)$  coincides with  $(0, \beta_0^\top)$  in the case of logistic link.

Real data. We apply train\_test\_split in scikit-learn (Pedregosa et al., 2011) on the whole dataset, and use the training split as the dataset  $z_{1:n}$ . We repeat this procedure 100 times to generate repetitions of  $z_{1:n}$ . For datasets with highly skewed responses or features, we apply stratified sampling on these variables. For yeast and wine, which have highly skewed multi-class categorical responses, we also remove classes with fewer than 3% of observations. Multinomial logistic regression on a small dataset with an extremely skewed response remains difficult with our method, as the design matrix tends to be ill-conditioned when applying the Bayesian bootstrap on x.

The training sets are split from the population set with stratification on all categorical and numerical variables with very low unique values. In certain datasets with heavily skewed numerical variables, we also stratify according to the 'bins' of these numerical variables. The bin boundaries are determined to ensure that each bin contains approximately the same number of data points. The number of bins depends on the datasets and is chosen such that the marginal distribution of the training set roughly matches that of the population set.

The details of the 19 real-world datasets are provided in Tables 3 and 4.

#### E.4 Constructions of credible sets

**Joint credible set** Let  $\widehat{\mu}$  and  $\widehat{\Sigma}$  denote the empirical mean and covariance estimated from the posterior draws  $\{\theta^{(l)}\}_{l=1}^L$ . For martingale posteriors, we use a diagonal covariance structure  $\widehat{\Sigma} = \operatorname{diag}(\widehat{\sigma}_1^2, \dots, \widehat{\sigma}_p^2)$  due to the limited number of posterior samples available for estimating a full covariance matrix. Our credible set is then:

$$\widehat{C}_{1-\alpha} = \Big\{ \theta : (\theta - \widehat{\mu})^{\top} \widehat{\Sigma}^{-1} (\theta - \widehat{\mu}) \le \widehat{r}_{1-\alpha}^2 \Big\},\,$$

where

$$\widehat{r}_{1-\alpha}^2 = \text{quantile}_{1-\alpha} \{ (\boldsymbol{\theta}^{(l)} - \widehat{\boldsymbol{\mu}})^\top \widehat{\boldsymbol{\Sigma}}^{-1} (\boldsymbol{\theta}^{(l)} - \widehat{\boldsymbol{\mu}}) \}_{l=1}^L,$$

is an empirical cutoff. This empirical-cutoff ellipsoid provides a data-driven approximation of the high-posterior density set without relying on  $\chi^2_{p,1-\alpha}$ , as stated in (12).

$\overline{z_{1:n}}$	Data ID	n	p	n/p	Population size	Num. classes	Num. cont. features	Num. cat. features
concrete	OpenML 44959	100	7	14.3	1030	0	8	0
quake	OpenML 550	50	4	12.5	2178	0	3	0
airfoil	OpenML $44957$	50	5	10.0	1503	0	5	0
energy	OpenML $44960$	50	6	8.3	768	0	8	0
fish	OpenML $44970$	50	6	8.3	908	0	6	0
kin8nm	OpenML $44980$	50	9	5.6	8192	0	8	0
auction	OpenML $44958$	50	11	4.5	2043	0	5	2
$\operatorname{grid}$	OpenML $44973$	50	12	4.2	10000	0	12	0
abalone	OpenML $45042$	20	5	4.0	4177	0	7	1
rice	UCI 545	100	4	25.0	3810	2	7	0
sepsis	OpenML 827	100	4	25.0	110341	2	2	1
banknote	OpenML 1462	100	4	25.0	1372	2	4	0
mozilla	OpenML 1046	100	5	20.0	15545	2	5	0
skin	OpenML $1502$	50	3	16.7	245057	2	3	0
blood	OpenML 1464	50	4	12.5	748	2	4	0
phoneme	OpenML 1489	50	6	8.3	5404	2	5	0
telescope	UCI 159	50	9	5.6	19020	2	10	0
yeast	OpenML 181	200	28	7.1	1350	5	8	0
wine	OpenML 40498	200	40	5.0	4873	5	11	0

Table 3: Details of the real-world datasets.

$z_{1:n}$	Target Name	Dropped features in the functional
concrete	strength	blast_furnace_slag, water
quake	$col\_4$	
airfoil	sound_pressure	angle_of_attack
energy	heating_load	relative_compactness, surface_area, roof_area
fish	LC50	MLOGP
kin8nm	y	
auction	verification.time	property.winner
$\operatorname{grid}$	stab	p1
abalone	Classnumberofrings	Length, Diameter, Whole_weight, Viscera_weight, Shell_weight
rice	Class	Area, Perimeter, Major_Axis_Length, Convex_Area
sepsis	hospital_outcome_1alive_0dead	
banknote	Class	V3
mozilla	state	start
$\operatorname{skin}$	Class	V2
blood	Class	V3
phoneme	Class	
telescope	class	fSize, fConc
yeast	$class\_protein\_localization$	erl, pox
wine	Class	V7, V8

Table 4: Target name and the features included in the functional of interest.

**Marginal credible interval.** Let  $\theta_j$  be the *j*-th dimension of  $\theta$ . The  $(1-\alpha)$  credible interval is computed from the empirical quantiles of its posterior draws:

$$\left[\text{quantile}_{\alpha/2}\{\theta_j^{(l)}\}_{l=1}^L, \text{ quantile}_{1-\alpha/2}\{\theta_j^{(l)}\}_{l=1}^L\right]. \tag{13}$$

# F Diagnostics

Tracking each dimension of  $\theta(F_N)$  as N grows is a common approach for diagnosing the convergence of  $\theta(F_N)$ . However, this becomes impractical when  $\theta$  is high-dimensional. Instead, we monitor convergence using the (scaled) expected  $L_1$ -norm between  $\theta(F_n)$  and  $\theta(F_N)$ :

$$\mathbb{E}_{F_N} \left[ \frac{1}{p} \| \theta(F_n) - \theta(F_N) \|_1 \right],$$

where  $p := \dim(\theta)$  and  $\theta(F_n)$  is the empirical risk minimiser (or maximum likelihood estimate of  $z_{1:n}$  in our experiment). In practice, we simulate many realisations of  $F_N$  to approximate this expectation. This expectation is shown in Figure 1 and corresponds to the blue trajectories in Figure 5. In addition to the expected value, we also present the  $L_1$ -norm for each realisation of  $F_N$  in Figure 5. While the paths corresponding to individual realisations of  $F_N$  exhibit variability, they generally stabilise as N increases, providing further empirical evidence that  $\theta(F_N)$  converges  $\mathbb{P}$ -a.s..

For completeness, we also provide trace plots for each dimension of  $\theta$  in the supplementary materials.

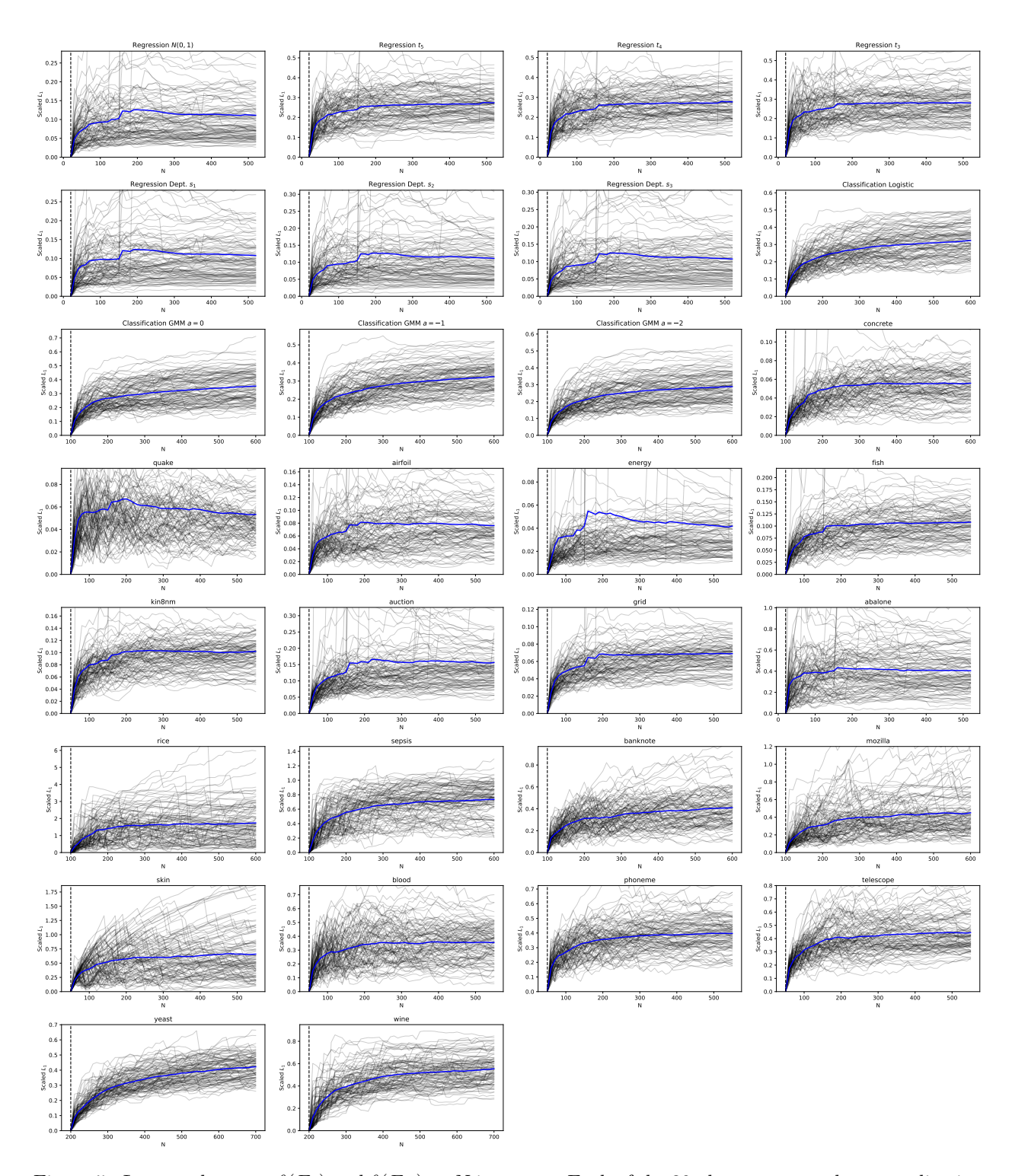


Figure 5:  $L_1$ -norm between  $\theta(F_n)$  and  $\theta(F_N)$  as N increases. Each of the 30 plots corresponds to a realisation  $z_{1:n}$  of a particular setup. Each of the grey lines corresponds to a realisation of  $F_N$ , and the blue lines are their average.

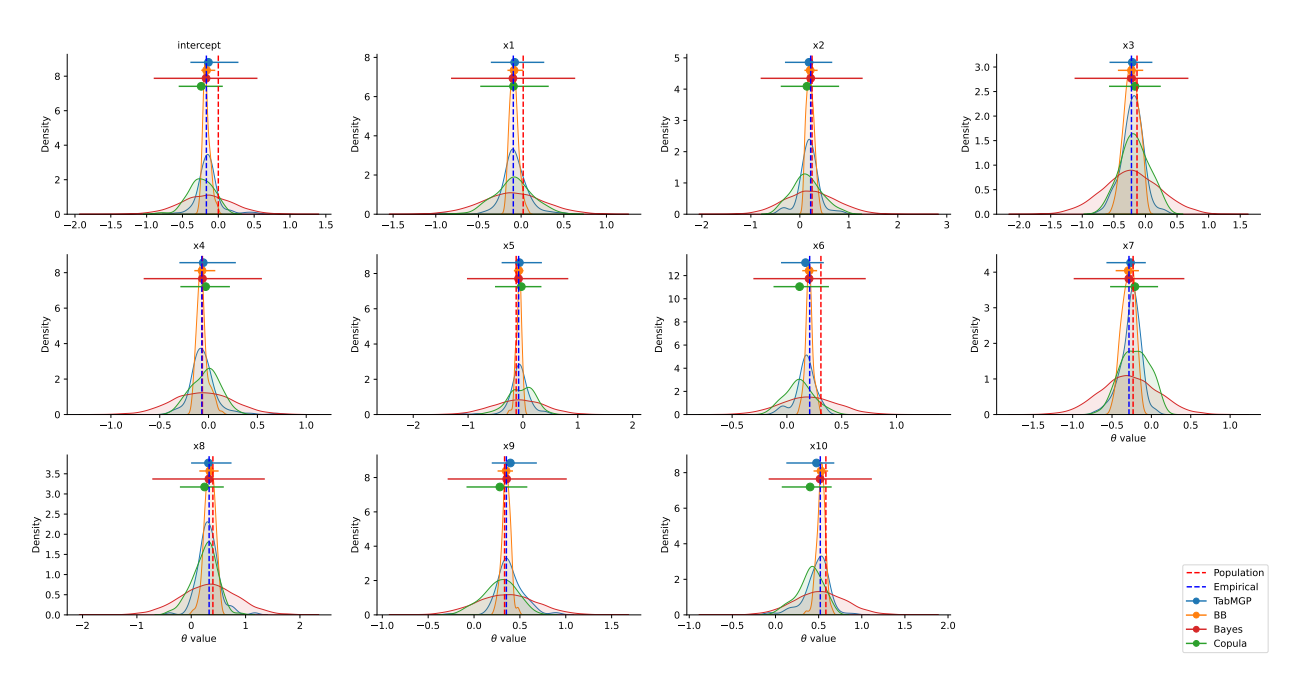


Figure 6: Marginal density plots of linear regression with the synthetic Gaussian i.i.d. data. For each posterior density, the 95% marginal credible interval is shown as a horizontal bar, and the posterior mean as dots. The vertical dotted red and blue lines correspond to  $\theta(F_0)$  and  $\theta(F_n)$ , respectively.

# G Marginal density and credible intervals of the posteriors

We present density plots of all posterior constructions for a single repetition of  $z_{1:n}$ . 95% marginal credible intervals are shown as coloured horizontal bars in each plot.

Due to space constraints, we display only the following setups: setups:

- 1. Linear regression with synthetic Gaussian i.i.d. data (Figure 6);
- 2. Logistic regression with synthetic Bernoulli data with a logistic link (Figure 7);
- 3. Linear regression with the 'abalone' dataset (Figure 8);
- 4. Logistic regression with the 'telescope' dataset (Figure 9);
- 5. Multinomial logistic regression with the 'yeast' dataset (Figure 10).

The density plots for the remaining setups are provided in the supplementary material.

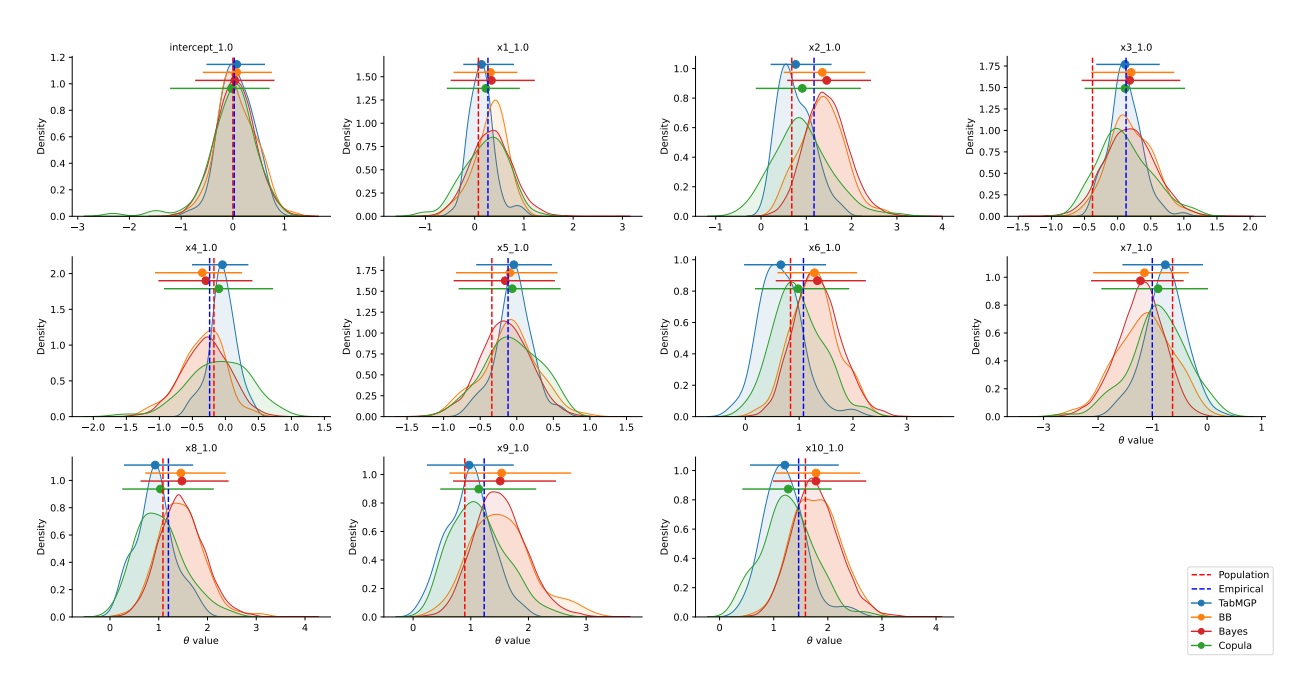


Figure 7: Marginal density plots of linear regression with the synthetic Bernoulli data with a logistic link. For each posterior density, the 95% marginal credible interval is shown as a horizontal bar, and the posterior mean as dots. The vertical dotted red and blue lines correspond to  $\theta(F_0)$  and  $\theta(F_n)$ , respectively.

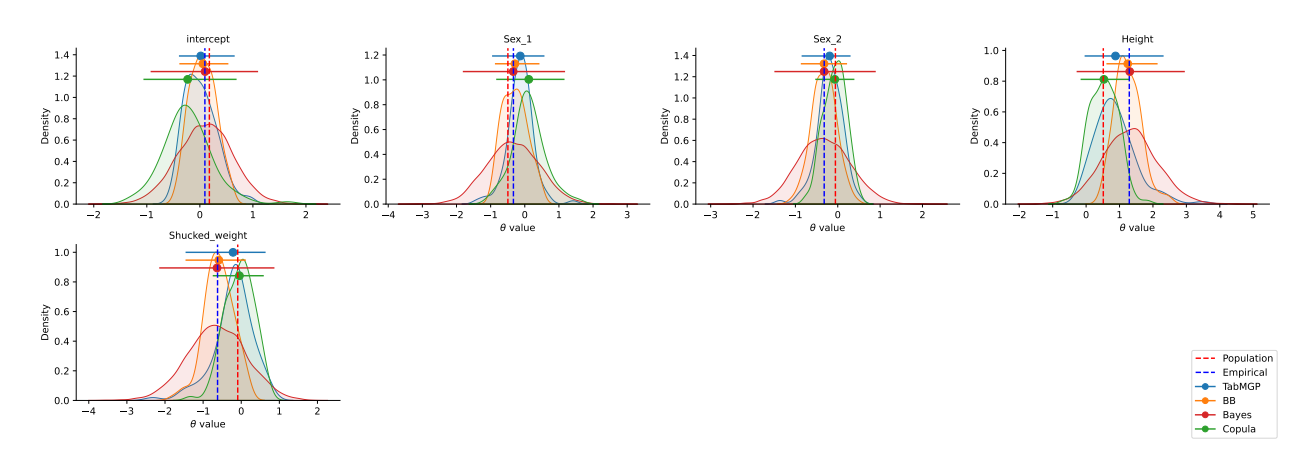


Figure 8: Marginal density plots for the 'abalone' dataset. For each posterior density, the 95% marginal credible interval is shown as a horizontal bar, and the posterior mean as dots. The vertical dotted red and blue lines correspond to  $\theta(F_0)$  and  $\theta(F_n)$ , respectively.

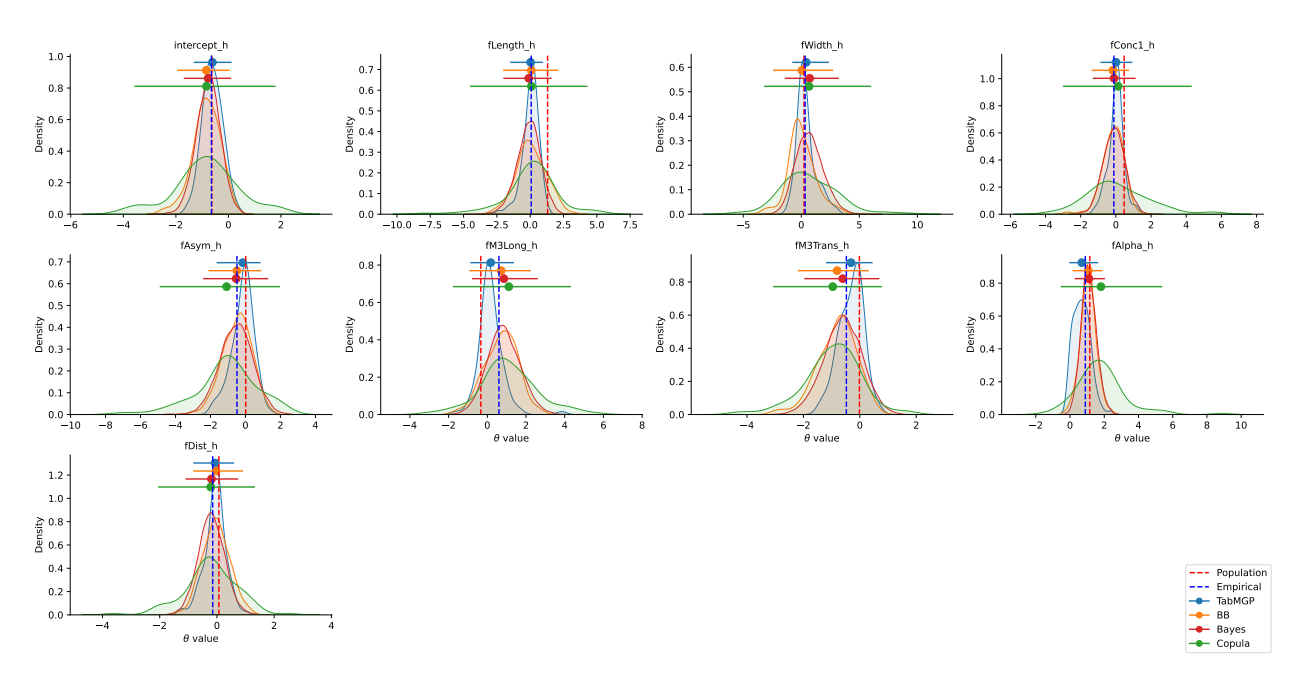


Figure 9: Marginal density plots for the 'telescope' dataset. For each posterior density, the 95% marginal credible interval is shown as a horizontal bar, and the posterior mean as dots. The vertical dotted red and blue lines correspond to  $\theta(F_0)$  and  $\theta(F_n)$ , respectively.

# H Coverage rate of the marginal credible interval

In addition to the joint credible sets discussed in the main text, we evaluate the performance of the 95% marginal credible intervals (13) for each parameter. Figure 11 shows boxplots of the marginal coverage rates for each method across all parameters in our experiments. While most methods' coverage is centered near the nominal 0.95 level, BB exhibits substantial under-coverage.

To jointly assess both coverage (calibration) and interval width (sharpness), we use the Winkler score (Winkler, 1972). For a  $(1 - \alpha)$  interval [l, u] and a true value  $\theta_0$ , the score is defined as:

$$W_{\alpha}(l, u, \theta_0) = (u - l) + \frac{2}{\alpha}(l - \theta_0)\mathbf{1}\{\theta_0 < l\} + \frac{2}{\alpha}(\theta_0 - u)\mathbf{1}\{\theta_0 > u\}.$$

The score penalises wide intervals and adds a larger penalty if the interval fails to cover the true value. A lower score indicates better performance.

The subsequent tables (Table 5 to Table 12) shows the empirical coverage and the median Winkler score (in parentheses) for each parameter, computed over 100 data realisations. The method with the lowest median Winkler score for each parameter is highlighted in bold. Summarising across all 30 setups and 293 individual parameters, TabMGP (TabPFN) achieves the best score 155 times, followed by Bayesian bootstrap (125), Copula (11), and the classical Bayesian posterior (2). TabPFN performs particularly well in logistic regression settings, while the Bayesian bootstrap is often competitive in linear regression, though its intervals frequently under-cover.

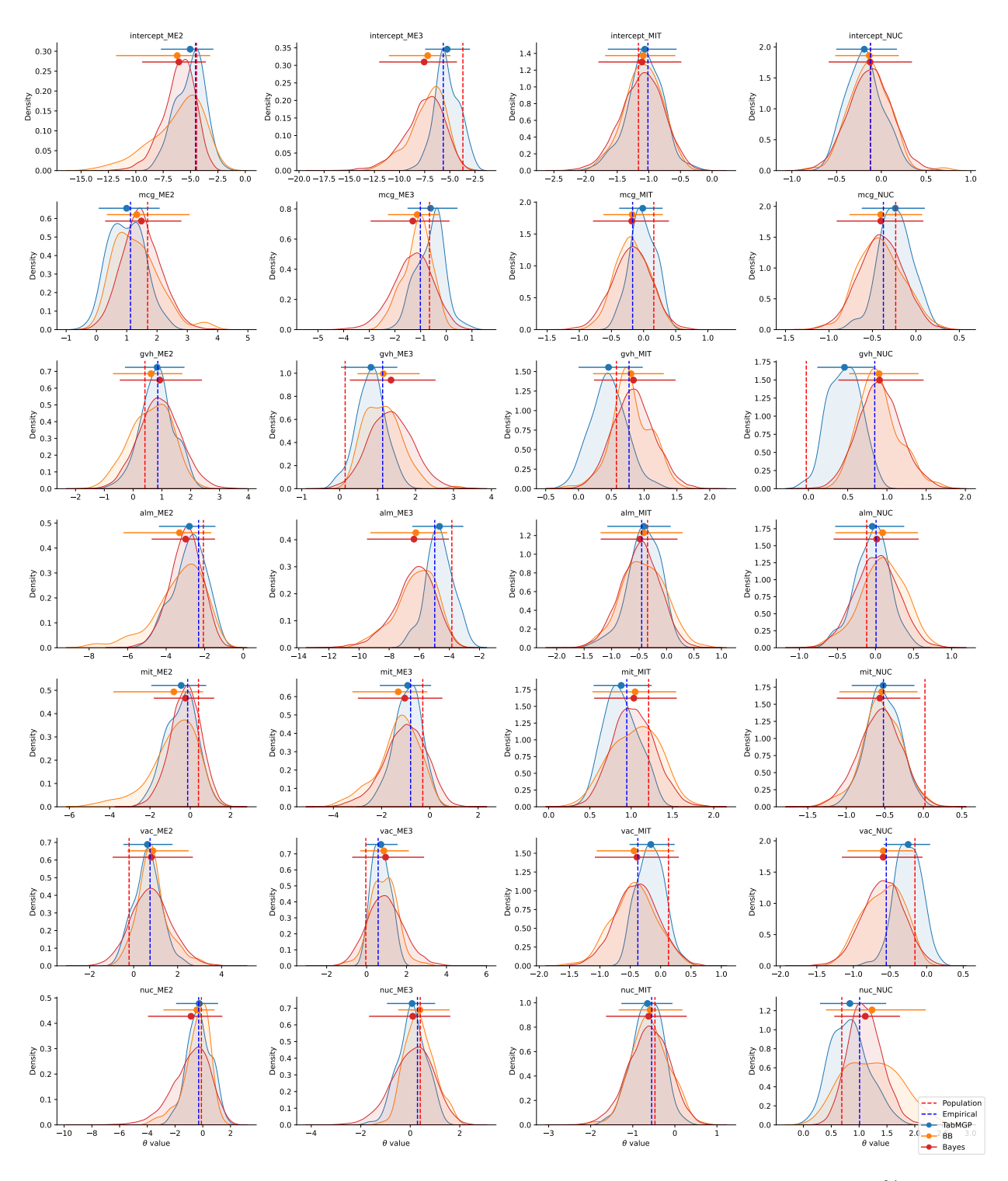


Figure 10: Marginal density plots for the 'yeast' dataset. For each posterior density, the 95% marginal credible interval is shown as a horizontal bar, and the posterior mean as dots. The vertical dotted red and blue lines correspond to  $\theta(F_0)$  and  $\theta(F_n)$ , respectively.

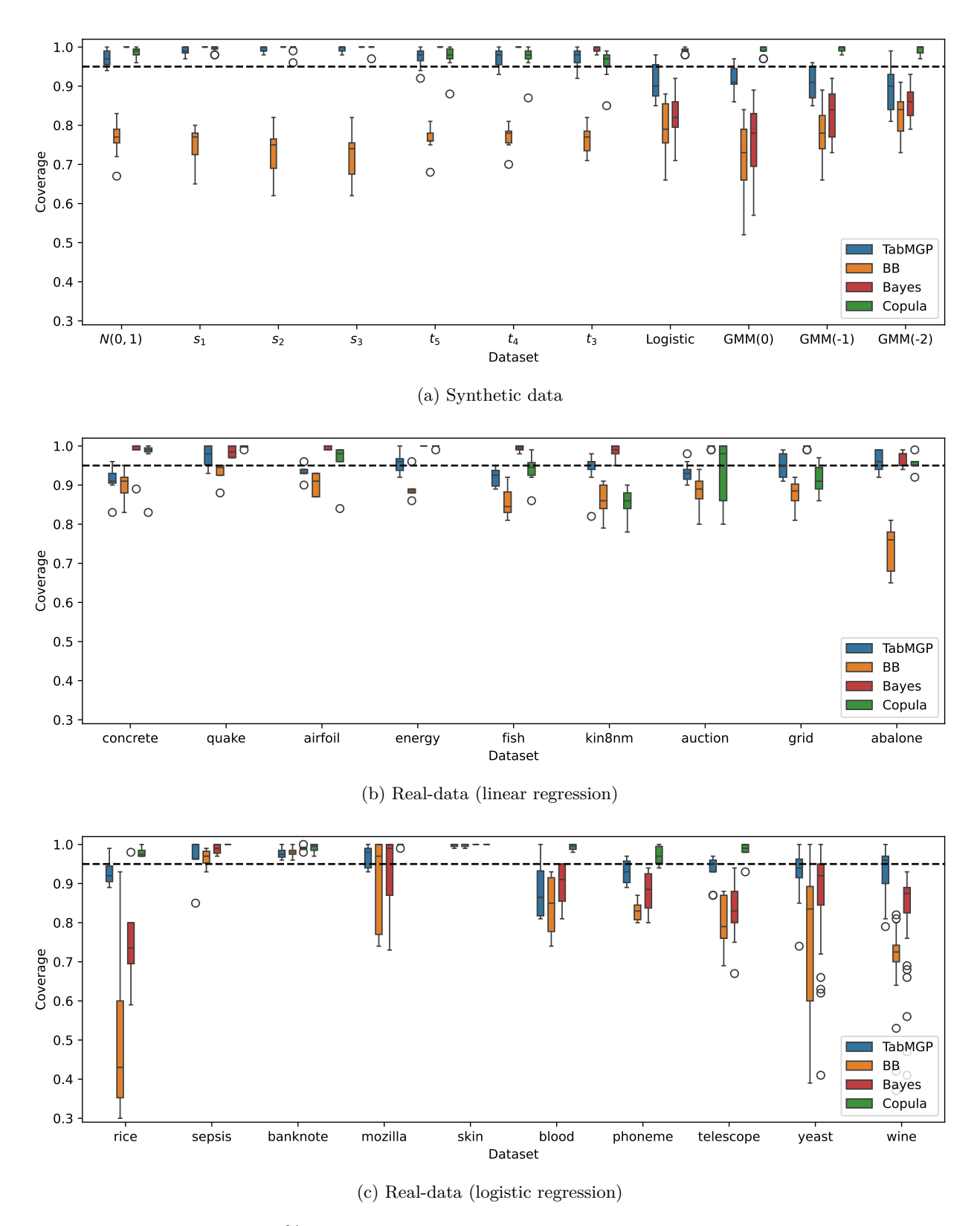


Figure 11: Coverage of the 95% marginal credible intervals. Each data point in the boxplots represents the coverage for a single dimension of  $\theta$  over 100 realisations of  $z_{1:n}$ .

$z_{1:n}$	Feature Name	TabMGP	BB	Copula	Bayes
	intercept	0.97(0.73)	0.83 (0.34)	1.00(0.63)	1.00(1.24)
	x1	1.00(0.64)	0.77 (0.38)	1.00(0.67)	1.00(1.34)
	x2	0.94  (0.68)	0.75 (0.37)	0.99(0.65)	1.00(1.26)
	x3	0.99(0.65)	0.76 (0.37)	0.99(0.65)	1.00(1.28)
	x4	0.99(0.64)	0.81 (0.36)	0.99(0.65)	1.00(1.28)
N(0, 1)	x5	0.99(0.66)	0.76 (0.38)	1.00(0.67)	1.00(1.29)
	x6	0.95(0.70)	0.72 (0.38)	0.97 (0.67)	1.00(1.30)
	x7	0.96 (0.69)	0.67 (0.39)	0.98(0.66)	1.00(1.23)
	x8	0.94(0.73)	0.78 (0.36)	0.96 (0.67)	1.00(1.27)
	x9	0.97 (0.71)	0.79 (0.36)	0.98(0.67)	1.00(1.26)
	x10	0.97  (0.80)	0.79(0.38)	0.98(0.63)	1.00(1.28)
	intercept	0.97 (0.80)	0.79 (0.40)	1.00 (0.65)	1.00 (1.24)
	x1	1.00(0.67)	0.78(0.43)	0.99(0.67)	1.00(1.33)
	x3	0.99(0.66)	0.76 (0.43)	1.00(0.65)	1.00(1.27)
	x4	1.00 (0.66)	0.77 (0.40)	0.97(0.66)	1.00(1.28)
	x5	0.99(0.67)	0.75 (0.42)	0.99(0.68)	1.00(1.28)
$t_5$	x6	0.98(0.75)	0.76 (0.46)	0.97(0.67)	1.00(1.29)
	x7	0.99(0.70)	0.78(0.42)	1.00(0.66)	1.00(1.23)
	x8	0.94(0.75)	0.68 (0.43)	0.97(0.66)	1.00(1.26)
	x9	0.97(0.75)	0.81 (0.41)	0.98(0.67)	1.00(1.26)
	x10	0.92  (0.86)	0.76 (0.44)	0.88(0.69)	1.00(1.28)
	intercept	0.97 (0.81)	0.81 (0.41)	1.00 (0.64)	1.00 (1.23)
	x1	1.00(0.68)	0.79(0.46)	0.99(0.67)	1.00(1.33)
	x2	0.94  (0.71)	0.76 (0.47)	0.96 (0.68)	1.00(1.25)
	x3	0.99(0.67)	0.78 (0.45)	1.00(0.65)	1.00(1.27)
	x4	1.00(0.68)	0.78 (0.43)	0.98(0.66)	1.00(1.29)
$t_4$	x5	0.99(0.67)	0.76 (0.45)	0.99(0.67)	1.00(1.28)
	x6	0.99(0.75)	0.75 (0.49)	0.97(0.67)	1.00(1.30)
	x7	0.98(0.72)	0.78 (0.43)	0.98(0.66)	1.00(1.24)
	x8	0.94(0.76)	0.70 (0.46)	0.97(0.65)	1.00(1.26)
	x9	0.97(0.74)	0.81 (0.43)	0.98(0.67)	1.00(1.27)
	x10	0.93(0.87)	0.75 (0.48)	0.87  (0.69)	1.00(1.28)
	intercept	0.97 (0.81)	0.82 (0.43)	0.96  (0.63)	0.99 (1.24)
	x1	1.00(0.68)	0.79(0.48)	0.99(0.66)	1.00(1.34)
	x2	0.95(0.70)	0.76 (0.49)	0.96(0.68)	1.00(1.25)
	x3	0.99(0.68)	0.78(0.49)	0.98(0.65)	0.99(1.27)
	x4	1.00(0.68)	0.78 (0.51)	0.98(0.66)	0.99(1.29)
$t_3$	x5	0.99(0.67)	0.73 (0.51)	0.98(0.66)	1.00(1.28)
	x6	0.98(0.73)	0.73 (0.54)	0.94(0.66)	0.98(1.33)
	x7	0.98(0.70)	0.77 (0.45)	0.98(0.65)	0.98(1.25)
	x8	0.92  (0.73)	0.71 (0.47)	0.93(0.65)	0.99(1.27)
	x9	0.98 (0.74)	0.79(0.45)	0.97(0.66)	1.00 (1.26)
	x10	0.93 (0.86)	$0.74_{(0.52)}$	0.85 (0.68)	1.00 (1.28)

Table 5: Coverage and Winkler score (median over 100 repetitions, shown in parantheses) of the marginal credible intervals for linear regression with synthetic i.i.d. data. The method with the lowest Winkler score is shown in bold. The target coverage is 0.95.

$z_{1:n}$	Feature Name	TabMGP	BB	Copula	Bayes
	intercept	0.99 (0.66)	0.79 (0.21)	1.00 (0.63)	1.00 (1.24)
	x1	1.00 (0.55)	0.73 (0.24)	1.00 (0.67)	1.00(1.34)
	x2	0.97(0.61)	0.73 (0.22)	1.00(0.65)	1.00(1.25)
	x3	1.00(0.59)	0.80 (0.22)	1.00(0.66)	1.00(1.27)
	x4	1.00(0.57)	0.77 (0.23)	1.00(0.66)	1.00(1.28)
$s_1$	x5	1.00(0.59)	0.77 (0.23)	1.00(0.66)	1.00(1.29)
	x6	0.98(0.64)	0.67 (0.25)	0.99(0.65)	1.00 (1.31)
	x7	0.99(0.59)	0.65 (0.25)	1.00(0.64)	1.00(1.23)
	x8	0.97(0.64)	0.72 (0.23)	0.98(0.67)	1.00(1.26)
	x9	0.99(0.62)	0.78(0.23)	1.00(0.66)	1.00 (1.27)
	x10	0.99(0.71)	0.78 (0.21)	0.98(0.64)	1.00(1.29)
	intercept	1.00(0.65)	0.82 (0.15)	1.00 (0.63)	1.00 (1.24)
	x1	0.99(0.55)	0.62 (0.24)	1.00(0.66)	1.00(1.34)
	x2	0.99(0.58)	0.78 (0.19)	1.00(0.65)	1.00(1.25)
	x3	1.00(0.55)	0.72 (0.19)	1.00(0.65)	1.00(1.27)
	x4	1.00(0.55)	0.76 (0.19)	1.00(0.67)	1.00(1.28)
$s_2$	x5	0.99(0.58)	0.76 (0.20)	1.00(0.67)	1.00(1.28)
	x6	1.00(0.61)	0.64 (0.22)	0.99(0.65)	1.00 (1.31)
	x7	0.99(0.57)	0.75 (0.18)	1.00(0.63)	1.00(1.24)
	x8	0.98(0.61)	0.66 (0.20)	1.00(0.66)	1.00(1.27)
	x9	1.00(0.60)	0.77 (0.18)	1.00(0.65)	1.00(1.26)
	x10	0.99 (0.70)	0.75 (0.18)	0.96 (0.64)	1.00 (1.28)
	intercept	1.00(0.63)	0.82 (0.14)	1.00(0.64)	1.00(1.23)
	x1	0.99(0.55)	0.62 (0.24)	1.00(0.66)	1.00(1.34)
	x2	0.98(0.59)	0.78 (0.17)	1.00(0.65)	1.00 (1.25)
	x3	0.99(0.56)	0.68 (0.18)	1.00(0.66)	1.00(1.27)
	x4	1.00(0.57)	0.69(0.21)	1.00(0.67)	1.00 (1.29)
$s_3$	x5	1.00(0.58)	0.75 (0.18)	1.00(0.67)	1.00 (1.29)
	x6	1.00(0.61)	0.62 (0.21)	1.00(0.65)	1.00(1.30)
	x7	1.00(0.56)	0.76 (0.17)	1.00(0.63)	1.00(1.23)
	x8	0.98(0.61)	0.67 (0.19)	1.00(0.66)	1.00 (1.27)
	x9	1.00(0.61)	0.74 (0.17)	1.00(0.66)	1.00(1.27)
	x10	0.99(0.71)	0.74 (0.18)	0.97(0.66)	1.00 (1.28)

Table 6: Coverage and Winkler score (median over 100 repetitions, shown in parantheses) of the marginal credible intervals for linear regression with synthetic, dependent-error data. The method with the lowest Winkler score is shown in bold. The target coverage is 0.95.

$\overline{z_{1:n}}$	Feature Name	TabMGP	BB	Copula	Bayes
	intercept_1.0	0.96 (1.11)	0.88 (1.40)	0.98 (1.67)	0.92 (1.46)
	$x1_{1.0}$	0.97 (0.97)	0.86 (1.45)	0.99(1.70)	0.87 (1.48)
	$x2_1.0$	0.85 (1.37)	0.76 (1.59)	0.98 (1.84)	0.79 (1.58)
	x3_1.0	0.95 (1.11)	0.81 (1.48)	1.00 (1.69)	0.85 (1.53)
	x4_1.0	0.98 (0.99)	0.85 (1.44)	0.99(1.71)	0.85 (1.49)
Logistic	$x5_{1.0}$	0.94 (1.05)	0.86 (1.47)	0.99(1.74)	0.88(1.50)
	$x6_{1.0}$	0.90(1.41)	0.77 (1.62)	1.00 (1.88)	0.80 (1.62)
	x7_1.0	0.89(1.31)	0.79(1.61)	1.00(1.85)	0.82 (1.58)
	$x8_{1.0}$	0.85 (1.59)	0.75 (1.84)	0.99(2.01)	0.81 (1.75)
	x9_1.0	0.89(1.58)	0.73 (1.70)	0.99(1.94)	0.76 (1.70)
	x10_1.0	0.86 (1.88)	0.66 (2.12)	0.99(2.26)	0.71 (2.05)
	${\rm intercept}\_1.0$	0.90 (1.54)	0.73 (2.09)	0.99 (2.18)	0.82 (2.06)
	$x1_{1.0}$	0.96 (1.21)	0.82 (1.90)	1.00 (1.98)	0.89(1.83)
	$x2_1.0$	0.86 (1.77)	0.70 (2.21)	0.97 (2.17)	0.77 (2.04)
	$x3_{1.0}$	0.91 (1.44)	0.79 (1.92)	0.99(1.96)	0.84 (1.87)
	x4_1.0	0.97 (1.26)	0.79 (1.85)	0.99(2.00)	0.79 (1.89)
GMM(0)	$x5_{1.0}$	0.94 (1.26)	0.84 (1.81)	0.97 (1.90)	0.87(1.86)
	$x6_{1.0}$	0.91 (1.96)	0.68 (2.51)	1.00(2.37)	0.70 (2.23)
	$x7_{1.0}$	0.93 (1.73)	0.74 (2.20)	0.99(2.11)	0.78 (2.05)
	$x8_{1.0}$	0.90(2.30)	0.62 (2.97)	0.99(2.51)	0.66 (2.52)
	x9_1.0	0.95 (1.94)	0.64 (2.79)	1.00(2.33)	0.69(2.38)
	x10_1.0	0.91 (2.74)	0.52  (3.92)	1.00(3.00)	0.57 (3.18)
	${\rm intercept}\_1.0$	0.96 (1.10)	0.89 (1.40)	0.98 (1.67)	0.92(1.46)
	x1_1.0	0.96 (0.96)	0.82(1.47)	1.00(1.68)	0.86 (1.52)
	$x2_{1.0}$	0.85 (1.33)	0.77 (1.59)	0.99(1.81)	0.84 (1.60)
	x3_1.0	0.91 (1.13)	0.83 (1.55)	0.99(1.68)	0.89(1.50)
	x4_1.0	0.96 (0.99)	0.82 (1.46)	0.99(1.69)	0.87 (1.48)
GMM(-1)	$x5_{1.0}$	0.93 (1.05)	0.88 (1.46)	1.00 (1.71)	0.90(1.50)
	$x6_{1.0}$	0.88 (1.43)	0.75 (1.64)	1.00(1.86)	0.81 (1.63)
	x7_1.0	0.85 (1.30)	0.78 (1.59)	1.00 (1.82)	0.83 (1.54)
	x8_1.0	0.86 (1.66)	0.68 (1.87)	0.99(2.05)	0.73 (1.79)
	x9_1.0	0.94 (1.48)	0.73 (1.74)	1.00 (1.92)	0.73 (1.71)
	x10_1.0	0.90 (1.81)	0.66 (2.06)	1.00 (2.25)	0.73 (2.02)
	${\rm intercept}\_1.0$	0.92 (1.06)	0.84 (1.37)	0.98  (1.68)	0.88(1.38)
	x1_1.0	0.97 (0.81)	0.89(1.24)	0.97 (1.57)	0.93 (1.32)
	$x2_{1.0}$	0.87 (1.00)	0.78 (1.30)	0.99(1.60)	0.83 (1.37)
	x3_1.0	0.94 (0.89)	0.88 (1.27)	0.97 (1.58)	0.89(1.33)
	x4_1.0	0.99(0.84)	0.91(1.24)	1.00(1.54)	0.92(1.32)
GMM(-2)	$x5_{1.0}$	0.90 (0.91)	0.82(1.32)	1.00(1.53)	0.86 (1.32)
	$x6_{1.0}$	0.91 (1.15)	0.84 (1.34)	1.00(1.67)	0.84 (1.40)
	$x7_{1.0}$	0.83 (1.04)	0.84(1.37)	1.00(1.61)	0.87 (1.34)
	x8_1.0	0.81 (1.33)	0.78 (1.43)	1.00(1.74)	0.82 (1.44)
	x9_1.0	0.83 (1.20)	0.79  (1.35)	1.00(1.65)	0.79 (1.41)
	x10_1.0	0.85 (1.53)	0.73 (1.57)	1.00(1.82)	0.80 (1.61)

Table 7: Coverage and Winkler score (median over 100 repetitions, shown in parantheses) of the marginal credible intervals for logistic regression with synthetic data. The method with the lowest Winkler score is shown in bold. The target coverage is 0.95.

$z_{1:n}$	Feature Name	TabMGP	BB	Copula	Bayes
~1.71	intercept	0.91 (0.29)	0.92 (0.26)	1.00 (0.55)	1.00 (0.40)
	cement	$0.91 (0.29) \\ 0.90 (0.33)$	0.92 (0.26) $0.91 (0.30)$	0.98 (0.50)	1.00 (0.40) $1.00 (0.48)$
	fly_ash	0.96 (0.33) $0.96 (0.34)$	0.91 (0.30) 0.92 (0.33)	0.98 (0.50) 0.99 (0.63)	0.99(0.50)
concrete	superplasticizer	0.90(0.34) $0.91(0.37)$	0.92 (0.33) 0.85 (0.36)	0.99 (0.63) 0.99 (0.49)	0.99(0.50) 0.99(0.51)
concrete	coarse_aggregate	0.91 (0.37) 0.91 (0.30)	0.83 (0.36) $0.91 (0.28)$	0.99 (0.49) 0.99 (0.47)	0.99(0.51) $0.99(0.43)$
	fine_aggregate	0.91 (0.30) 0.95 (0.29)	0.91 (0.28) 0.95 (0.27)	0.99(0.47) $1.00(0.45)$	0.99(0.43) $1.00(0.44)$
		$0.93 (0.29) \\ 0.83 (0.36)$	0.93 (0.27) $0.83 (0.36)$		0.89(0.44)
	age			0.83 (0.34)	
	intercept	0.96 (0.48)	0.95(0.51)	1.00(1.02)	1.00(0.56)
quake	$col\_1$	1.00(0.23)	0.88(0.48)	0.99(0.50)	1.00(0.63)
quare	$col\_2$	0.93 (0.25)	0.94(0.52)	1.00(0.80)	0.97 (0.57)
	$col\_3$	1.00 (0.24)	0.95  (0.50)	1.00(0.81)	0.97  (0.58)
	intercept	0.93 (0.42)	0.93 (0.37)	0.99 (0.63)	0.99 (0.57)
	frequency	0.90(0.50)	0.87 (0.46)	0.84(0.51)	0.99(0.63)
airfoil	chord_length	0.96(0.45)	0.91 (0.39)	0.98(0.55)	1.00(0.59)
	free_stream_velocity	0.94(0.40)	0.93 (0.36)	0.99(0.55)	0.99(0.57)
	$displacement\_thickness$	0.93(0.46)	0.87 (0.41)	0.96(0.59)	1.00(0.60)
	intercept	0.92 (0.29)	0.88 (0.15)	1.00 (0.45)	1.00 (0.58)
	wall area	1.00 (0.25)	$0.96_{(0.12)}$	1.00 (0.35)	1.00 (0.62)
	overall height	0.97(0.26)	0.89(0.15)	1.00 (0.49)	1.00 (0.59)
energy	orientation	0.96(0.25)	0.88 (0.16)	1.00 (0.34)	1.00 (0.58)
	glazing area	0.93(0.26)	0.86 (0.16)	1.00 (0.34)	1.00 (0.60)
	glazing_area_distribution	$0.96  {\scriptstyle (0.25)}$	0.89 (0.16)	0.99 (0.33)	1.00 (0.59)
	intercept	0.93 (0.45)	0.83 (0.37)	0.99 (0.54)	1.00 (0.58)
	CICO	0.89 (0.49)	0.86 (0.46)	0.86  (0.52)	0.99(0.63)
	SM1_Dz	0.89 (0.50)	0.83 (0.42)	0.92 (0.50)	0.98 (0.64)
fish	GATS1i	0.92 (0.42)	0.92 (0.35)	0.96 (0.47)	1.00 (0.58)
	NdsCH	0.95(0.46)	0.81 (0.42)	0.95 (0.46)	1.00(0.64)
	NdssC	0.94 (0.49)	0.89(0.47)	0.94 (0.49)	0.99(0.68)
	intercept	0.94 (0.48)	0.91 (0.39)	0.90 (0.36)	1.00 (0.60)
	theta1	0.96(0.40)	0.85 (0.40)	0.86 (0.37)	0.99(0.63)
	theta2	0.98(0.41) $0.98(0.40)$	0.86 (0.40)	0.88 (0.36)	1.00 (0.61)
	theta3	0.96  (0.40) $0.96  (0.52)$	0.90(0.40) $0.90(0.37)$	0.78 (0.36)	0.99(0.61)
kin8nm	theta4	0.96  (0.43)	0.90(0.37) $0.90(0.39)$	0.90 (0.35)	1.00 (0.60)
	theta5	0.82  (0.49)	0.87 (0.41)	0.86 (0.35)	0.98 (0.61)
	theta6	0.02 (0.49) $0.92 (0.43)$	0.79(0.41)	0.78 (0.36)	0.95 (0.61) $0.95 (0.61)$
	theta7	0.94 (0.43) 0.94 (0.42)	0.13(0.42) $0.84(0.40)$	0.84 (0.36)	0.98(0.61) $0.98(0.61)$
	theta8	0.94 (0.42) 0.96 (0.41)	0.84 (0.40)	0.84 (0.36) $0.87 (0.36)$	0.93(0.61) $0.97(0.61)$
	0110000	0.30 (0.41)	0.04 (0.40)	0.01 (0.30)	0.01 (0.01)

Table 8: Coverage and Winkler score (median over 100 repetitions, shown in parantheses) of the marginal credible intervals for linear regression with real data. The method with the lowest Winkler score is shown in bold. The target coverage is 0.95.

$z_{1:n}$	Feature Name	TabMGP	BB	Copula	Bayes
	intercept	0.93 (0.75)	0.89 (0.55)	1.00 (1.70)	1.00 (1.24)
	$property.product\_2$	0.91 (1.41)	0.87 (1.17)	0.84 (1.71)	0.99(1.81)
	$property.product\_3$	0.93(1.07)	0.89(0.88)	0.80(1.73)	1.00(2.08)
	property.product_4	0.96(1.06)	0.89(0.87)	0.88(1.51)	1.00(2.02)
	property.product $\_5$	0.94(1.16)	0.89 (0.91)	0.97 (1.73)	1.00(2.32)
auction	property.product_6	0.94(1.00)	0.93 (0.79)	0.82 (1.61)	1.00 (1.91)
	process.b1.capacity	0.98(0.50)	0.94 (0.42)	1.00(1.04)	1.00(0.72)
	process.b2.capacity	0.90(0.40)	0.80 (0.35)	1.00(0.84)	0.99(0.64)
	process.b3.capacity	0.92  (0.35)	0.94 (0.27)	0.98(0.67)	1.00(0.69)
	process.b4.capacity	0.93(0.40)	0.86 (0.33)	1.00(1.20)	1.00(0.64)
	property.price	0.91(0.46)	0.81 (0.41)	1.00(1.03)	1.00(0.73)
	intercept	0.92 (0.41)	0.91 (0.31)	0.86 (0.34)	1.00 (0.63)
	tau1	0.91(0.40)	0.81 (0.31)	0.91(0.32)	1.00(0.63)
	tau2	0.94(0.40)	0.89 (0.31)	0.89(0.33)	1.00(0.62)
	tau3	0.91(0.39)	0.86 (0.31)	0.90(0.34)	1.00(0.62)
	tau4	0.94(0.40)	0.89 (0.31)	0.91(0.33)	0.99(0.63)
ani d	p2	0.97(0.37)	0.90(0.30)	0.96(0.35)	1.00(0.63)
grid	p3	0.99(0.36)	0.91 (0.30)	0.97(0.34)	1.00(0.63)
	p4	0.99(0.38)	0.87 (0.30)	0.97(0.34)	1.00(0.62)
	g1	0.92(0.40)	0.82 (0.32)	0.86(0.34)	0.99(0.63)
	g2	0.98(0.40)	0.88 (0.31)	0.94(0.34)	1.00(0.63)
	g3	0.96(0.40)	0.86 (0.31)	0.89(0.34)	1.00(0.64)
	g4	0.98(0.40)	0.92 (0.31)	0.93(0.35)	1.00(0.63)
	intercept	0.94 (1.24)	0.76 (1.23)	0.99 (1.79)	0.98 (1.76)
	$\text{Sex}\_1$	0.92  (1.83)	0.78 (1.78)	0.95 (1.88)	0.98(2.72)
abalone	$Sex\_2$	0.99(1.48)	0.81 (1.70)	0.95(1.58)	0.99(2.31)
	Height	0.99(1.54)	0.65(1.76)	0.96 (1.37)	0.94 (2.20)
	Shucked_weight	0.96 (1.42)	0.68 (1.61)	0.92 (1.54)	0.95 (2.01)

Table 9: Coverage and Winkler score (median over 100 repetitions, shown in parantheses) of the marginal credible intervals for linear regression with real data. The method with the lowest Winkler score is shown in bold. The target coverage is 0.95.

$z_{1:n}$	Feature Name	TabMGP	BB	Copula	Bayes
rice	intercept_Osmancik Minor_Axis_Length_Osmancik Eccentricity_Osmancik Extent_Osmancik	$0.89(2.72)\\0.93(3.91)\\0.91(5.36)\\0.99(1.21)$	0.30 (14.3) 0.49 (7.81) 0.37 (20.1) 0.93 (2.18)	0.97 (6.22) 0.97 (11.2) 0.98 (14.5) 1.00 (4.14)	0.59 (3.48) 0.74 (5.20) 0.73 (7.45) 0.98 (2.12)
sepsis	intercept_1 sex_0male_1female_1_1 age_years_1 episode_number_1	1.00 (1.77) 1.00 (1.73) 0.85 (2.00) 1.00 (1.19)	0.98 (2.91) 0.99 (3.59) 0.96 (2.69) 0.93 (2.57)	1.00 (6.42) 1.00 (7.84) 1.00 (4.88) 1.00 (3.28)	0.97 (3.24) 1.00 (4.00) 0.98 (3.24) 1.00 (3.53)
banknote	intercept_2 V1_2 V2_2 V4_2	1.00 (1.33) 0.96 (2.24) 0.97 (2.26) 0.98 (2.01)	1.00 (1.44) 0.96 (2.63) 0.98 (2.50) 0.98 (2.26)	1.00 (1.45) 1.00 (2.85) 0.97 (2.46) 0.99 (2.31)	1.00 (1.52) 0.99 (3.06) 0.99 (2.57) 0.98 (2.05)
mozilla	intercept_1 id_1 end_1 event_1 size_1	0.94 (1.44) 0.99 (0.77) 0.98 (1.00) 1.00 (0.78) 0.93 (4.13)	$\begin{array}{c} 0.77 (1.77) \\ 1.00 (0.91) \\ 0.97 (1.11) \\ 1.00 (0.92) \\ 0.74 (5.06) \end{array}$	1.00 (2.40) 1.00 (1.83) 1.00 (2.08) 1.00 (2.05) 0.99 (4.43)	0.87 (1.58) 1.00 (0.96) 0.99 (1.08) 1.00 (1.00) 0.73 (4.33)
skin	intercept_2 V1_2 V3_2	1.00 (1.70) 1.00 (3.00) 0.99 (2.91)	1.00 (1.85) 1.00 (3.29) 0.99 (3.18)	1.00 (2.11) 1.00 (3.23) 1.00 (3.37)	1.00 (2.89) 1.00 (2.49) 1.00 (2.85)
blood	intercept_2 V1_2 V2_2 V4_2	1.00 (1.48) 0.82 (2.07) 0.91 (2.50) 0.81 (2.10)	0.93 (2.15) 0.91 (2.66) 0.74 (3.73) 0.79 (2.89)	1.00 (3.68) 0.98 (4.18) 0.99 (4.99) 1.00 (4.01)	0.95 (2.03) 0.95 (2.55) 0.81 (3.38) 0.87 (2.95)
phoneme	intercept_2 V1_2 V2_2 V3_2 V4_2 V5_2	$\begin{array}{c} 0.97(1.73) \\ 0.96(1.93) \\ 0.95(1.85) \\ 0.90(1.93) \\ 0.91(1.71) \\ 0.89(1.45) \end{array}$	0.83 (1.98) 0.85 (2.15) 0.87 (2.33) 0.80 (2.47) 0.80 (1.97) 0.83 (1.95)	1.00 (3.37) 1.00 (3.58) 0.98 (3.44) 0.96 (3.70) 0.95 (3.70) 0.94 (3.32)	0.91 (2.35) 0.94 (2.97) 0.93 (2.35) 0.83 (2.30) 0.80 (1.97) 0.86 (1.76)
telescope	intercept_h fLength_h fWidth_h fConc1_h fAsym_h fM3Long_h fM3Trans_h fAlpha_h fDist_h	$\begin{array}{c} 0.97(1.93) \\ 0.87(5.08) \\ 0.95(4.47) \\ 0.95(2.64) \\ 0.96(2.58) \\ 0.95(2.52) \\ 0.97(2.21) \\ 0.87(2.56) \\ 0.93(2.12) \end{array}$	0.88 (2.73) 0.69 (7.01) 0.70 (6.45) 0.76 (3.63) 0.78 (3.42) 0.87 (3.81) 0.88 (3.12) 0.79 (3.04) 0.81 (2.96)	1.00 (7.44) 0.98 (13.4) 0.98 (11.9) 0.99 (9.79) 1.00 (7.77) 0.99 (7.24) 1.00 (6.63) 0.93 (8.26) 0.98 (6.56)	0.94 (2.63) 0.67 (6.61) 0.80 (6.27) 0.81 (3.27) 0.88 (3.67) 0.87 (3.71) 0.90 (3.21) 0.75 (2.61) 0.83 (2.67)

Table 10: Coverage and Winkler score (median over 100 repetitions, shown in parantheses) of the marginal credible intervals for logistic regression with real data. The method with the lowest Winkler score is shown in bold. The target coverage is 0.95.

$z_{1:n}$	Feature Name	TabMGP	BB	Bayes
	intercept_ME2	0.89 (6.53)	0.39 (53.6)	0.41 (42.0)
	$intercept\_ME3$	0.95 (3.53)	0.54 (6.47)	0.66 (5.32)
	$intercept\_MIT$	0.97 (1.08)	0.87 (1.33)	0.92(1.47)
	$intercept\_NUC$	1.00(0.70)	1.00(0.81)	1.00(0.90)
	$mcg\_ME2$	0.90(3.02)	0.61 (5.43)	0.63 (3.86)
	$mcg\_ME3$	0.92 (1.67)	0.82 (2.18)	0.92(2.43)
	$mcg\_MIT$	0.90(0.90)	0.90(1.13)	0.98(1.28)
	$mcg\_NUC$	0.96 (0.67)	0.94 (0.90)	0.98(0.96)
	$gvh\_ME2$	0.94(2.46)	0.56 (7.29)	0.83 (4.09)
	$gvh\_ME3$	0.94(1.42)	0.82 (2.24)	0.94(2.28)
	$gvh\_MIT$	0.92 (0.96)	0.86 (1.25)	0.95(1.34)
	$gvh\_NUC$	0.94 (0.61)	0.93  (0.86)	0.96(0.94)
	$alm\_ME2$	0.93 (3.53)	0.47 (12.2)	0.72 (4.91)
wonat	$alm\_ME3$	0.95 (3.20)	0.56 (5.97)	0.62 (4.24)
yeast	$\operatorname{alm}_{-}\operatorname{MIT}$	0.85 (1.22)	0.89(1.50)	0.91 (1.50)
	$alm\_NUC$	0.93  (0.82)	0.90  (0.99)	0.98(1.13)
	$\mathrm{mit}\_\mathrm{ME2}$	0.93 (2.50)	0.57 (5.91)	0.89(4.13)
	$\mathrm{mit}\_\mathrm{ME3}$	0.97 (1.99)	0.84 (2.76)	0.92  (3.07)
	$\operatorname{mit} \operatorname{MIT}$	0.87 (0.93)	0.84 (1.10)	0.90  (1.09)
	$\operatorname{mit}$ _NUC	0.93 (0.77)	0.90(0.95)	0.94 (1.03)
	$vac\_ME2$	0.99(2.07)	0.63 (3.67)	0.88(3.66)
	$vac\_ME3$	0.97 (1.63)	0.87 (2.35)	0.94(2.80)
	$vac\_MIT$	0.98(0.76)	0.90(1.08)	0.97 (1.14)
	$vac\_NUC$	0.95 (0.54)	0.89(0.75)	0.94  (0.83)
	$\mathrm{nuc}\_\mathrm{ME2}$	0.98(3.40)	0.55 (7.57)	0.94 (6.30)
	$\mathrm{nuc}\_\mathrm{ME3}$	0.74 (1.79)	0.74 (2.42)	0.85(2.68)
	$\mathrm{nuc}\_\mathrm{MIT}$	0.94 (1.35)	0.83 (1.69)	0.95(1.87)
	nuc_NUC	0.89 (0.88)	0.81 (1.09)	0.81 (0.99)

Table 11: Coverage and Winkler score (median over 100 repetitions, shown in parantheses) of the marginal credible intervals for multinomial logistic regression with the 'yeast' data. The method with the lowest Winkler score is shown in bold. The target coverage is 0.95.

$z_{1:n}$	Feature Name	TabMGP	BB	Bayes
	intercept_3	0.97 (2.87)	0.42 (12.1)	0.47 (6.82)
	$intercept\_4$	0.99(2.90)	0.37 (18.9)	0.41 (12.2)
	$intercept\_5$	0.98(3.00)	0.53 (8.18)	0.56 (4.96)
	$intercept\_6$	0.99(3.97)	0.81 (9.82)	0.89(7.39)
	V1_3	0.97 (1.23)	0.72 (2.49)	0.89 (2.35)
	V1_4	0.90(1.31)	0.74 (2.39)	0.85 (2.35)
	V1_5	0.88(1.41)	0.74 (2.51)	0.89 (2.50)
	V1_6	0.91 (1.81)	0.74 (3.37)	0.84  (3.55)
	V2_3	0.90 (1.16)	0.79 (2.14)	0.89 (2.04)
	$V2\_4$	0.81 (1.43)	0.73 (2.25)	0.88 (2.09)
	$V2\_5$	0.82 (1.62)	0.69(2.42)	0.87 (2.36)
	V2_6	0.84 (2.12)	0.67 (3.61)	0.80(3.39)
	V3_3	0.96 (1.15)	0.76 (2.62)	0.90(2.43)
	V3_4	0.97 (1.20)	0.72 (2.63)	0.90(2.43)
	V3_5	0.99(1.37)	0.80(2.74)	0.90(2.67)
	V3_6	1.00 (1.85)	0.74  (3.62)	0.89(3.79)
	V4_3	0.98(1.50)	0.70 (2.95)	0.88(3.06)
	V4_4	0.96 (1.55)	0.74 (2.94)	0.91 (2.99)
	V4_5	0.93 (1.77)	0.72 (3.07)	0.89(3.21)
wine	V4_6	0.90(2.19)	0.71 (4.52)	0.84 (4.32)
wille	V5_3	0.98(1.34)	0.68 (2.77)	0.90(3.06)
	$V5\_4$	0.96 (1.39)	0.77(3.00)	0.88(3.11)
	V5_5	0.94 (1.99)	0.82  (3.26)	0.93  (3.68)
	V5_6	0.97(2.49)	0.74 (5.15)	0.90(5.41)
	V6_3	0.79(2.07)	0.69(3.86)	0.69(3.05)
	$V6\_4$	0.84 (2.04)	0.70(3.73)	0.66 (3.08)
	V6_5	0.84 (2.19)	0.72 (3.78)	0.68(3.16)
	V6_6	0.83 (2.72)	0.70 (4.75)	0.76 (3.89)
	V9_3	0.97 (1.31)	0.75 (2.89)	0.84 (2.65)
	V9_4	0.98(1.35)	0.72 (2.96)	0.84 (2.63)
	V9_5	0.95 (1.48)	0.71 (3.05)	0.83 (2.76)
	V9_6	0.94  (1.82)	0.73 (3.85)	0.81 (3.74)
	V10_3	0.97 (1.25)	0.75 (2.47)	0.86 (2.54)
	V10_4	0.96  (1.28)	0.71 (2.63)	0.92(2.54)
	V10_5	0.96 (1.38)	0.74 (2.54)	0.87 (2.63)
	V10_6	0.96 (1.64)	0.79(3.44)	0.87 (3.33)
	V11_3	0.93 (1.95)	0.77 (3.01)	0.93(3.22)
	V11_4	0.97 (1.99)	0.73  (3.24)	0.89(3.24)
	V11_5	0.93 (2.17)	0.71 (3.29)	0.88(3.37)
	V11_6	0.93 (2.88)	0.64 (4.51)	0.76 (4.47)

Table 12: Coverage and Winkler score (median over 100 repetitions, shown in parantheses) of the marginal credible intervals for multinomial logistic regression with the 'wine data. The method with the lowest Winkler score is shown in bold. The target coverage is 0.95.